

Geometric and kinematic controls on the internal structure of a large normal fault in massive limestones: The Maghlaq Fault, Malta

C.G. Bonson¹, C. Childs, J.J. Walsh*, M.P.J. Schöpfer, V. Carboni²

Fault Analysis Group, School of Geological Sciences, University College Dublin, Belfield, Dublin 4, Ireland

Received 5 September 2005; received in revised form 12 June 2006; accepted 30 June 2006

Available online 26 December 2006

Abstract

The Maghlaq Fault is a large, left-stepping normal fault (displacement >210 m) cutting the Oligo-Miocene pre- to syn-rift carbonates of SW Malta. Two principal slip zones separate the deformed rocks of the fault zone from the undeformed wall rocks. Fault rocks derived from fully lithified, pre- to early syn-rift sediments comprise relatively continuous fine-grained veneers of cataclasite and localised fault-bound lenses of wall rock, occurring over a range of scales, which are commonly brecciated. The lenses result from the linkage of slip surfaces, the inclusion of asperities and the formation of Riedel shears within the fault zone. In contrast, fault rock incorporated from unlithified syn-rift sediments comprise relatively continuous veils of rock that deformed in a ductile manner. Anomalously thick parts of the fault zone with highly complex structure and content are associated with breached relay zones, branch-lines and bends; these structures represent progressive stages of fault segment linkage. The progressive evolution and bypassing of fault zone complexities to form a smoother and more continuous active fault surface, results in complex fault rock distributions within the fault zone. Segment linkage structures have high fracture densities which combined with their significant vertical extents suggest they are potentially important up-fault fluid flow conduits.

© 2006 Published by Elsevier Ltd.

Keywords: Branch-line; Fault zone; Fluid flow; Relay; Segment linkage

1. Introduction

An appreciation of the spatial heterogeneity of fault zones is a prerequisite for constructing conceptual models of fault zone structure and is fundamental to an understanding of the mechanical and hydrological behaviour of faults. Despite the importance of outcrop-scale observational constraints, few detailed studies of the 2-D and 3-D structure of normal fault zones within carbonate successions dominated by massive limestones are available within the published literature. This paucity of data is partly attributable to the difficulty of

identifying and examining faults within thick and homogeneous limestone sequences and to the often relatively poor preservation potential of faults in limestones, sometimes arising from the operation of karstic processes. In this article, we provide a detailed description of the internal architecture of the Maghlaq Fault, a normal fault zone in southwest Malta, which offsets a Tertiary pre- to syn-rift carbonate succession by a minimum of 210 m. There is near-continuous exposure of the footwall to the Maghlaq Fault over a 4 km long coastal outcrop. The hangingwall is preserved for 2.5 km and coastal inlets provide numerous cross-sections through the fault zone. Detailed field mapping on to aerial photographs was carried out at 1:4000 and, locally, at 1:200 scales to characterise the heterogeneity in structure and content of the Maghlaq Fault zone.

The tectonic setting and stratigraphic framework of the study area are outlined in the following section. A summary of the main characteristics of the Maghlaq Fault is then

* Corresponding author. Tel.: +353 1 716 2606; fax: +353 1 716 2607.

E-mail address: john@fag.ucd.ie (J.J. Walsh).

¹ Present address: SRK Consulting (Canada), Suite 800, 1066 West Hastings Street, Vancouver, British Columbia, V6E 3X2, Canada.

² Present address: Alcan Inc., 1188 Sherbrooke Street West, Montreal, Québec, H3A 3G2, Canada.

followed by a consideration of the along strike variability of the basic structure and content of the fault zone and the nature of the fault rocks. Building on the description of the basic fault zone structure, we then describe several large-scale fault complexities that represent elements of anomalous fault zone structure; namely relay zones, branch-lines and bends. These structures are considered in terms of the fault zone processes active during growth of the Maghlaq Fault. Finally, we discuss the structure of the Maghlaq Fault in terms of the generic permeability structure of fault zones in carbonate successions and speculate about the potential implications for subsurface fluid flow.

2. Geology of the Maghlaq Fault

2.1. Tectonic setting

The Maltese Islands are situated on the northern flank of the ESE–WNW striking Pantelleria Rift system (Reuther and Eisbacher, 1985), also known as the Strait of Sicily Rift (Finetti, 1982; Cello et al., 1985). The Pantelleria Rift is an elongate fault-controlled trough within the foreland of the Sicilian Apennine-Maghrebian thrust and fold belt (Hill and Hayward, 1988; Pedley, 1990) (Fig. 1). The largest faults in the Pantelleria Rift accommodate throws of >2 km (Fig. 2) and are associated with the development of a stepped seafloor topography and the opening of three exceptionally deep troughs: the Malta Trough, the Linosa Trough and the Pantelleria Trough, in which the seafloor bathymetry exceeds 1 km in depth (Jongsma et al., 1985). The major development of the Pantelleria Rift took place during Plio-Quaternary times, when displacement rates far outstripped sedimentation rates within the central parts of the basin (Dart et al., 1993). The

uplift of the northern rift flank (i.e., the present-day Maltese Archipelago) from the Miocene onwards, together with a falling sea-level, resulted in the emergence of the islands during early Messinian times (Pedley, 1987a).

The Maghlaq Fault has a maximum displacement of >210 m, making it the largest displacement fault outcropping in the archipelago. In contrast to the majority of faults in Malta which strike ENE–WSW, the Maghlaq Fault strikes ESE–WNW (Fig. 2) and is the only major fault of the Maltese Islands with a Pantelleria Rift trend (Figs. 1 and 2). Although the two sets of faults are nearly orthogonal, analysis of fault-related changes in sediment thickness, imaged on offshore 2-D seismic data, reveals a shared four stage tectono-sedimentary history for the Miocene–Quaternary Periods (Fig. 3), as follows: (a) pre-rift phase (>21 Ma); (b) early syn-rift phase (21–6 Ma) characterised by minor fault-controlled thickness changes and the development of neptunian dykes; (c) late syn-rift phase (<5 Ma) during which major fault growth took place and localised basin depocentres and areas of non-deposition evolved; and (d) post-rift phase (probably <1.5 Ma; Dart et al., 1993).

2.2. Stratigraphic framework

The stratigraphy of the Maltese Graben system consists of five main litho-stratigraphic units that represent a relatively simple Oligo-Miocene pre- to syn-rift succession (Fig. 3; Pedley, 1990; Dart et al., 1993). The nature of the individual formations, their moderate thickness changes and lateral variations across the islands have been documented by previous workers (e.g. Pedley et al., 1976; Pedley, 1978, 1987a,b, 1990, 1996, 1998; Bennett, 1980; Pedley and Bennett, 1985). At the base of the exposed succession are the Oligocene (Chattian) Lower Coralline Limestones, which can be up to 1000 m thick (Pedley et al., 1976), although only the uppermost 140 m are exposed in the Maltese Archipelago (Fig. 3). The outcropping limestones predominantly comprise pale yellow biomicrites at their lowermost exposures, conformably overlain by massively bedded coralline algal limestones, representing sedimentation in restricted gulf to open-marine conditions (Pedley, 1978). Near the top of the succession, deposition in a shallow marine shoal environment gave rise to cross-bedding of coarse bioclastic limestones (Pedley et al., 1976).

Overlying the Lower Coralline Limestone is the Aquitanian to Serravallian age Globigerina Limestone Formation (Fig. 3), a relatively uniform succession of yellow to grey-white coloured, biomicritic wackestones and marls that may attain thicknesses of >200 m. These limestones largely consist of massive units of poor-moderately consolidated planktonic foraminifera (globigerina) and pteropods (Pedley, 1978) and represent a deepening to outer shelf conditions (Bennett, 1980). Occasional marker horizons occur in the form of brown phosphoritic conglomeratic layers (<0.7 m in thickness) which overlay well-developed hardgrounds (Pedley and Bennett, 1985).

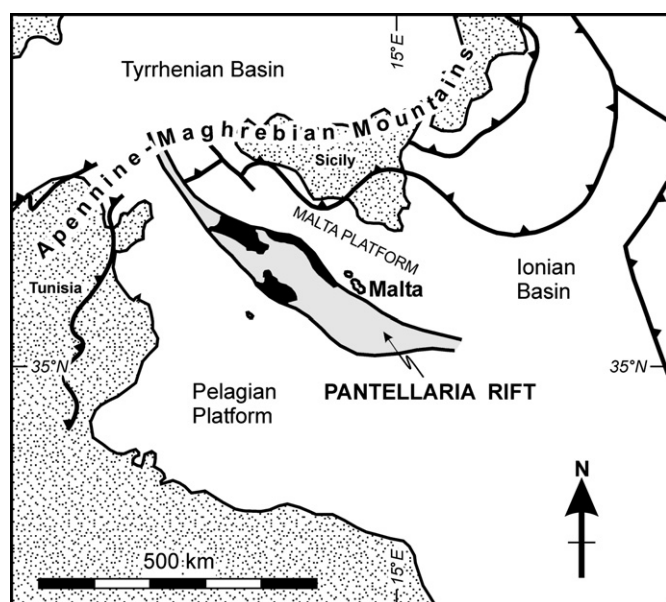


Fig. 1. Map of the central Mediterranean region showing the location of the Maltese archipelago with respect to the Pantelleria Rift and Maghrebian Apennine thrust and fold belt (after Dart et al., 1993).

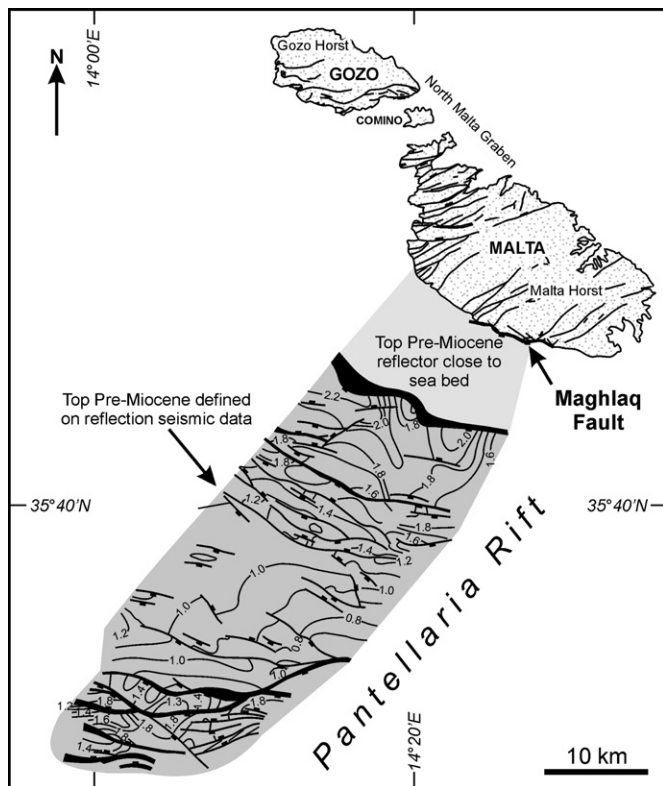


Fig. 2. Map showing the locations of major normal faults in the Maltese islands together with an interpretation of 2-D seismic lines from the northern part of the Pantelleria Rift, both from Dart et al. (1993). The Maghlaq Fault is located on the SW coast of Malta and represents the most northerly extent of the Pantelleria Rift fault trend. Horizon contoured for two-way time (seconds; $1 \text{ s} \approx 1 \text{ km}$).

A major lithological transition occurs at the top of the Globigerina Limestone, where biomicrites grade over 1 m into globigerinid marls at the base of the Blue Clay Formation (Fig. 3). On Malta, the Blue Clay comprises up to 65 m of pale grey-green banded clays which predominantly consist of kaolinite and glauconite, with <30% carbonate material (Pedley et al., 1976; Pedley and Bennett, 1985). The Blue Clay is interpreted as sediment deposited within an open muddy marine environment with water depths of about 150 m during the mid- to late Serravalian (Pedley et al., 1976). Capping the Blue Clay, is a very poorly cemented, dark blue-green bioclastic glauconitic limestone known as the Greensand Formation (Pedley, 1978), which is rarely greater than 1 m thick throughout Malta. The presence of intense bioturbation within this Tortonian age unit indicates that it was deposited in shallow marine conditions (Pedley et al., 1976; Dart et al., 1993).

The uppermost outcropping unit of the Maltese stratigraphy is the Late Tortonian to Messinian age Upper Coralline Limestone Formation (Fig. 3). The succession comprises three depositional units which show a transition from coralline algal biostrome facies at the base to coral and algal patch reefs and finally to platform and slope facies at the top of the formation (Bosence and Pedley, 1982; Pedley, 1987b). These represent the principal syn-faulting depositional packages which

show marked changes in both facies-type and thickness across the fault (Dart et al., 1993).

The flat-lying footwall outcrops predominantly consist of massive Lower Coralline Limestone, which varies from a hard, low porosity/low permeability mudstone (Maghlaq Member), to bioclastic wackestones and packstones (Xlendi and Attard Members; Pedley, 1993). Inland, the Lower Coralline Limestone is capped by the Globigerina Limestone, and in sporadic flat-topped hills the remainder of the Miocene strata is preserved. Local stratigraphic thickness determinations derived from the footwall succession are given in Fig. 3.

The hangingwall of the Maghlaq Fault, exposed over the westernmost 2.5 km of the fault outcrops, predominantly consists of well-bedded calciturbidites and inter-sand shoals belonging to the Upper Coralline Limestone (Dart, 1991). The absence of exposures of pre-rift strata in the hangingwall precludes the determination of absolute displacements. However, on the basis of stratigraphic thicknesses within the direct footwall of the fault local to Ghar Lapsi, a minimum displacement of 210 m can be calculated (Figs. 3 and 4).

2.3. Timing and conditions of faulting

Using fault-related stratigraphic thickness changes identified on 2-D seismic data, Dart et al. (1993) proposed two periods of normal fault activity in the Pantelleria Rift: (a) an early syn-rift phase (21–6 Ma); and (b) a late syn-rift phase (<5 Ma; Fig. 3). The early and late syn-rift sediment packages in the Pantelleria Rift are approximately 4 and 9 times thicker, respectively, than onshore Malta. Across the Maghlaq Fault, sequence thickening and associated variations in sedimentary facies of the Upper Coralline Limestone Formation reflect Tortonian-Lower Messinian age displacements of the late syn-rift phase (Pedley, 1987b; Dart et al., 1993). Burial of the underlying lithologies in the hangingwall, precludes the confirmation of a probable early syn-rift movement history.

The most recent age for significant displacements on the Maghlaq Fault is given by late Pleistocene-Holocene age alluvial fan conglomerates (Pedley, 1993), which overlie an erosion surface at several places along the fault scarp. Where the fans cross the fault, they are offset by a few tens of centimetres. Neotectonic fault movements along the Maghlaq Fault or other faults in the Maltese Archipelago have not been reported.

Although thick post-Miocene marine successions are found offshore (Dart et al., 1993), Pliocene sediments are absent onshore, and thin, patchy Quaternary marine deposits are restricted to the northwest and southeast extremes of Malta. The presence of caves and karstic surface depressions containing Pleistocene bones of land-dwelling mammals (Pedley et al., 1976) and the lack of significant sediment thicknesses suggest that, similar to the Hyblean Mountains of SE Sicily, post-Messinian Malta remained emergent to the present day (Marty Pedley, written communication, 2002). Based on the total thickness of the exposed footwall stratigraphy above the level of the present-day outcrop of the Maghlaq Fault

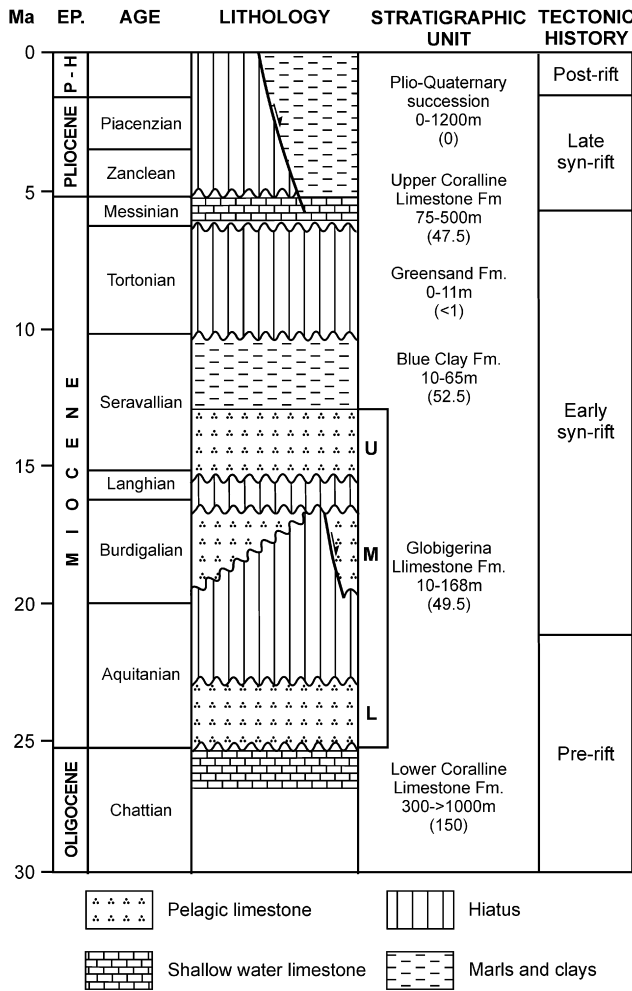


Fig. 3. Tectono-stratigraphic log of the Oligocene–Quaternary age sediments of the Maltese archipelago (modified from Dart et al., 1993). Stratigraphic thickness ranges are given for onshore Malta and values in parentheses are local thicknesses, measured by Pedley (1993) from the mapped geology in the footwall of the Maghlaq Fault. EP. denotes ‘Epoch’, with P-H representing Pleistocene to Holocene series, which is otherwise referred to as Quaternary in the text.

(Fig. 3), the burial depth during the Miocene is therefore unlikely to have been more than 300 m.

Previous studies have highlighted the importance of pressure solution as a deformation mechanism in fault zones in limestones, particularly during fault nucleation (Odonne and Massonnat, 1992; Willemse et al., 1997; Peacock et al., 1998; Graham et al., 2003). The lack of any discernible structures indicative of pressure solution processes (e.g. stylolites and veins) along the Maghlaq Fault is attributed to faulting at a very shallow crustal level.

3. Main characteristics of the Maghlaq Fault

The overall geometry of the Maghlaq Fault is that of a left-stepping, en échelon normal fault array. Relatively straight, 1–2 km long fault segments, which strike ESE–WNW and dip 60–75° SSW, have orthogonal separations of 50–400 m

(Fig. 4). These segments are linked (or in some cases are conjectured to link offshore) by short sections of the fault that strike approximately E–W or ENE–WSW, forming fault bends at Ix-Xaqqa, Ras Hanzir and Ras il-Hamrija (Fig. 4).

The Maghlaq Fault zone, *sensu stricto*, is a clearly defined zone of intensely deformed rocks, 5–40 m wide, separated from less deformed hangingwall and footwall rocks by a pair of major slip zones. The hangingwall bounding slip zone is marked by strongly sheared Upper Coralline Limestone sediments, ranging from 2 to 10 m in thickness, containing a fault-parallel planar foliation defined by elongate ribbons of fine and coarse-grained sediment. The footwall fault zone boundary is defined by planar, polished Lower Coralline Limestone slip surfaces, coated with a veneer of fine-grained cataclasite (Sibson, 1977). Movement striations, corrugations and polish marks on the footwall slip surface and on internal fault-bound lenses range in pitch from 75° ESE to perfectly dip-parallel, indicating that the normal displacement has a minor sinistral component.

Between Ix-Xaqqa and Ghar Lapsi, the hangingwall bedding dips 10–20° S and is cut by several antithetic and synthetic faults (Fig. 5a; section A–A’). Antithetic faults terminate into a distributed zone of ductile deformation where they approach the main fault zone. This geometry is consistent with the Upper Coralline Limestone being unlithified, or partially lithified, at the time of deformation (Maltman, 1994). Towards the east, the dip of the hangingwall bedding steepens to about 40° S, due to normal drag along the fault. This steepening is accompanied by increasing structural complexity of the hangingwall. At In-Neffiet (Fig. 4), the sediments are locally overturned, dipping sub-vertically towards the north and are displaced by a north-dipping low-angle thrust fault. Similar deformation has been recorded in the hangingwalls of growth faults in the Gulf of Suez rift (Gawthorpe et al., 1997). The presence of a recumbent fold in moderately inclined hangingwall calci-turbidites at Il-Miqtub (Fig. 4) suggests that drag along the fault resulted in a southward dipping topography, causing local gravity collapse and slumping of unconsolidated Upper Coralline Limestone sediments.

4. Fault rock types and distributions

To record the along strike variation in the internal architecture of the fault zone, sections were constructed at nine stations by projecting data from cliff sections and exposures within gullies over strike-parallel distances of 1–100 m on to vertical planes (Fig. 5). The locations of sections (Fig. 5a) allow the principal characteristics and internal variability of the fault zone to be assessed on a lateral scale of tens to hundreds of metres.

Fault rocks derived from each offset stratigraphic unit, from the Lower Coralline Limestone to the Upper Coralline Limestone, are observed along the studied outcrops. The different fault rocks are stacked in the stratigraphic order of their parent wall rocks, although the fault rock stratigraphy is rarely complete. Fault rocks occur mainly as extensive sheets covering large parts of the fault surface or occur within, or associated

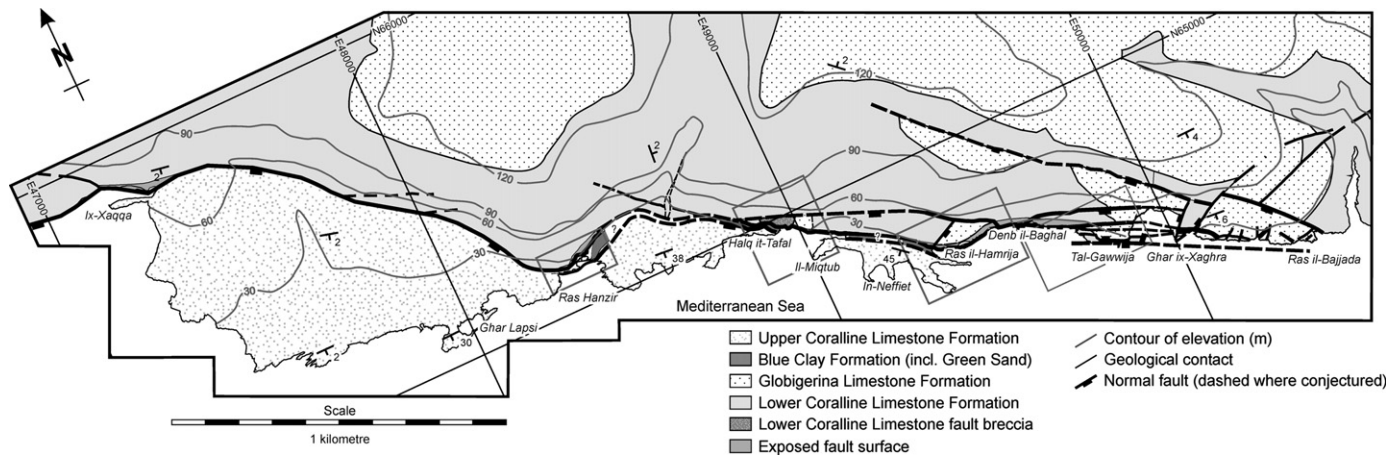


Fig. 4. Geological map of the Maghlaq Fault study area. Individual members of the stratigraphic formations are not distinguished on the map. Topographic contour intervals are in metres above sea level. Grid references are in UTM coordinates (datum: WGS84, projection: NUTM33).

with, well-defined lenses. The type and distribution of fault rock varies between the different source lithologies. Here we describe the character, typical occurrence and variability in thickness of the fault rock components derived from each of the four offset units in stratigraphic order. The spatial variation of the different fault rock components is illustrated schematically in Fig. 6. The largest fault zone thickness variabilities can be related to large-scale (>100 m) irregularities in the fault trace, which are described in a later section.

4.1. Lower Coralline Limestone

The immediate footwall of the Maghlaq Fault is cut by mm-scale offset deformation bands oriented sub-parallel to the main fault (Fig. 7a). The deformation bands occur in arrays extending up to 15 m into the footwall, with the highest frequencies of bands occurring closest to the principal fault. Analysis of the spacings of the deformation bands indicates that they are uniformly distributed, with mean frequencies of 6–17 per metre. The arrays contain clusters 0.1–0.2 m wide, where deformation band frequencies reach 55 per metre. The $\pm 20^\circ$ variability in the strike of the deformation bands, coupled with their close spacing, results in a high degree of connectivity.

Individual deformation bands are generally <1.5 mm wide and are defined by a zone of comminuted angular bioclasts within a micritic matrix, bounded on one or both sides by a connected system of discrete shears (Fig. 7a). Cataclasis of the moderately porous Lower Coralline Limestone results in a decrease of the porosity of the limestone within the deformation bands, in the same manner as occurs within deformation bands in high porosity sandstones (Aydin and Johnson, 1978).

Deformation band arrays are absent or very poorly developed over significant areas of exposed limestone in the direct footwall of the Maghlaq Fault. The widest arrays occur at Il-Miqtab (≥ 15 m wide; Fig. 5a; section F–F') and Ras il-Hamrija (15 m wide; Fig. 5a; section G–G'), where a large lens of Lower Coralline Limestone is bounded by two principal traces of the Maghlaq Fault (Fig. 4) that are relatively closely spaced (approximately 60 and 85 m respectively). These wide deformation

band arrays reflect the higher internal strains of the lens, which is also shown by a small rotation (<5°) of bedding in sympathy to the fault displacement (i.e. towards the SSW).

The footwall slip surface of the Maghlaq Fault is a pronounced, and frequently cliff-forming, polished and striated surface (Fig. 7b). Beneath the fault surface is a hard, very fine-grained, low-porosity cataclasis up to 30 mm thick that has a sharp contact with the parent rock (Fig. 7c). Fault breccia, as defined by Sibson (1977), is rare within the fault zone but occurs particularly at branch-lines between slip surfaces (Fig. 6). The breccias are moderately-strongly cohesive and range from coarse breccias, containing cm-scale highly angular clasts (Fig. 7d), to microbreccias containing sub-angular to sub-rounded fragments. All breccias exhibit a moderate to high porosity.

Lens-shaped slivers of intact Lower Coralline Limestone occur within the fault zone (Figs. 6 and 8a). The preserved lenses, which have strike-parallel lengths of 3 to 40 m, are derived from the footwall. Limited measurements of the dimensions of these lenses from the Maghlaq Fault and smaller faults elsewhere in Malta indicate that the average lens length is about 11 times the thickness, and the dip dimensions are 1.2 to 2.2 times the length.

Moderate internal deformation of the lenses, principally that of progressive flattening and elongation parallel to fault dip, is accommodated by steep, sometimes oversteepened (and therefore thrust-like), Riedel shears (Fig. 8b). Additionally, localised internal shear strain, in sympathy with the fault displacements, is accommodated by intense microfracturing. This type of deformation has only been detected in lenses containing rare, less competent beds within the Lower Coralline Limestone. Lenses become brecciated or are intensely fractured by minor faults, where they taper to a thickness of a few decimetres at their fringes (Fig. 8c). The lateral fringes of the lenses, which represent minor branch-lines within the fault array where slip surfaces coalesce, are generally oriented parallel or sub-parallel to the slip direction (Fig. 8a and c).

For a given field measurement of the total fault zone thickness, the thickness of individual lithological components can be compared to a predicted thickness, T_{LITH} , based on the

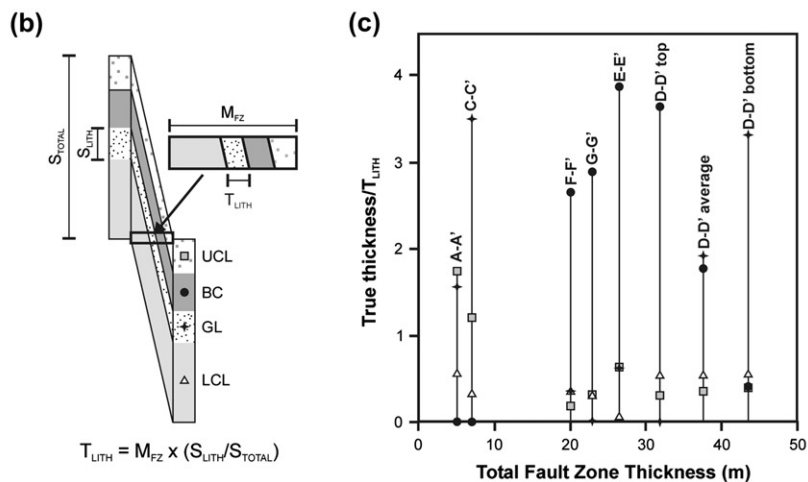
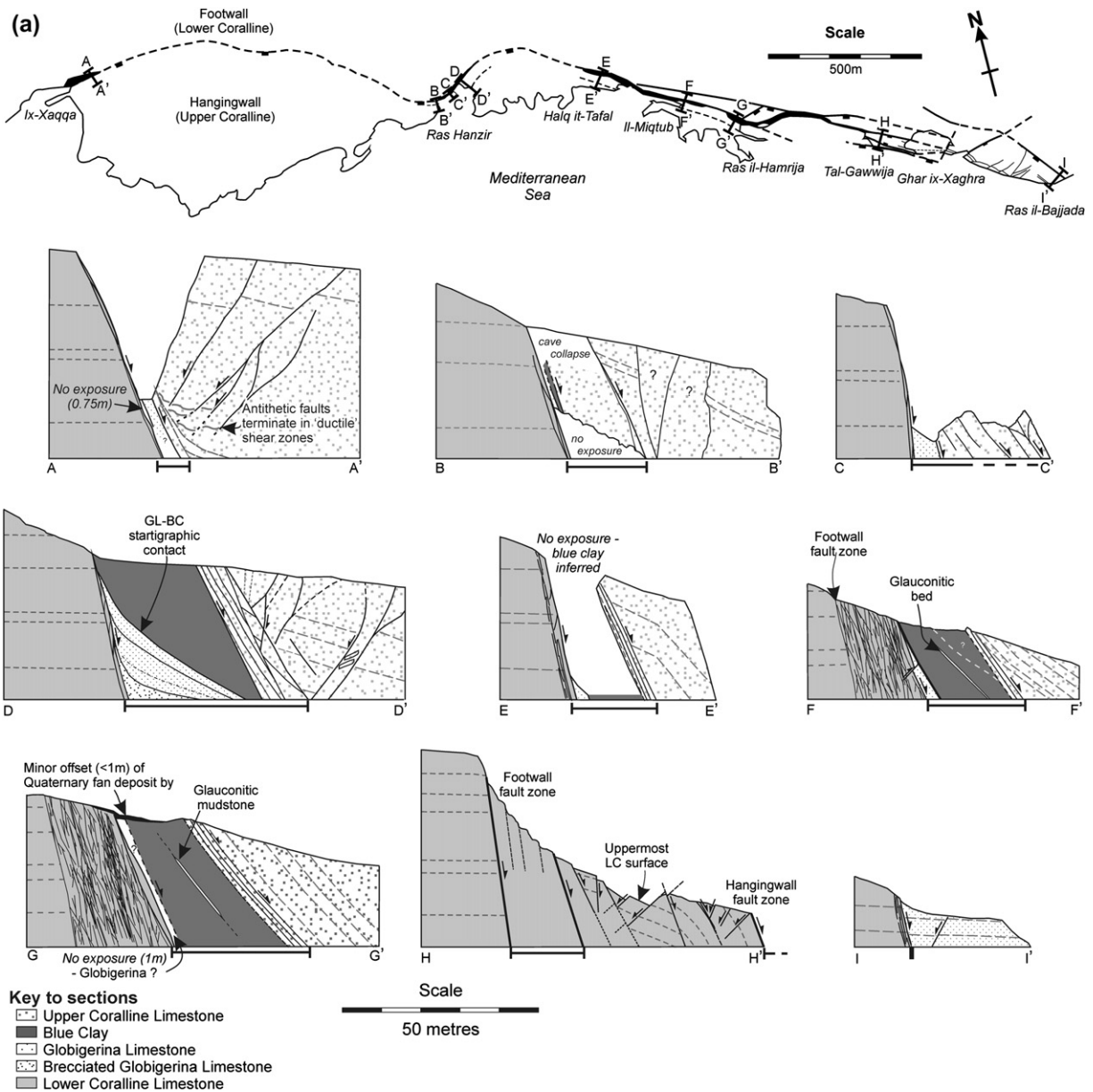


Fig. 5. (a) Simplified map of the Maghlaq Fault zone indicating positions of fault zone sections A–A' to I–I'. The fault zone, defined by well-defined shear boundaries, is indicated beneath each section by a bar. (b) Schematic diagram illustrating parameters used to calculate predicted fault zone lithology thickness, T_{LITH} . (c) Plot of true thickness/predicted thickness for each fault zone lithology versus total fault zone thickness measured in the field. Section C–C' is not represented due to uncertainty regarding the maximum fault zone thickness at this locality.

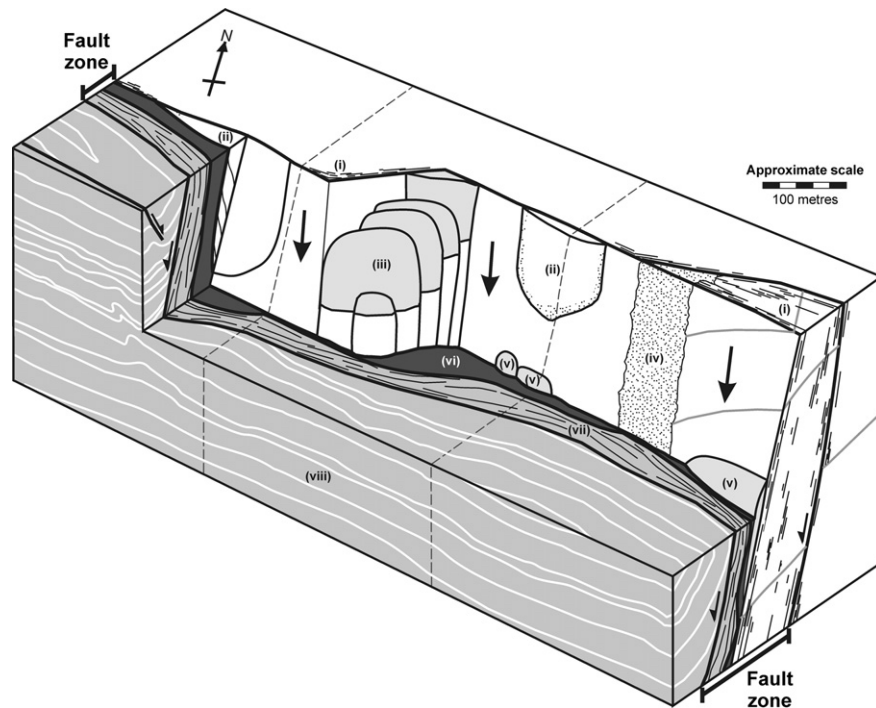


Fig. 6. Schematic 3-D diagram illustrating the main characteristics of the internal structure of the Maghlaq Fault zone at the current exposure level. The principal features illustrated are as follows: (i) Footwall Lower Coralline Limestone is relatively undeformed outside the fault zone, apart from areas close to the fault that are sporadically affected by arrays of deformation bands, particularly near fault irregularities. (ii) Lenses of footwall Lower Coralline Limestone are incorporated into the fault zone. The lenses typically show internal deformation by Riedel shears and they are intensely brecciated where they thin towards their margins. (iii) Overlapping lenses of footwall-derived limestone are formed by the mechanical attrition of an angular bend (formerly a branch-line). (iv) Intensely brecciated footwall limestone defines a branch-line between major fault segments. (v) Discontinuous lenses of deformed Globigerina Limestone. (vi) Blue Clay fault zone component is characterised by rapid thickness changes but relatively high continuity within the fault zone. (vii) Highly continuous hangingwall shear zone comprising deformed Upper Coralline Limestone. (viii) Moderately dipping hangingwall Upper Coralline Limestones contain slumps and minor antithetic faults. It should be noted that the fault slip direction is slightly oblique to the dip direction, as indicated by the small disparity in the arrows (slip direction) and the dashed lines (dip direction) on the fault surface. Although an approximate scale is presented, the structures shown can occur over a range of scales within an individual fault system.

assumptions that all lithologies displaced past a point contribute equally to the fault zone and displacement is constant along the fault trace, as depicted in Fig. 5b. Although an over-simplification, this analysis highlights the variability of fault zone components. Notably it shows that where the fault zone is very thick, Lower Coralline fault products (lenses, breccia and cataclasite) occur on all outcrops of the Maghlaq Fault (Fig. 5c), but in general only ever comprise up to 25% of the total fault zone content, even though Lower Coralline Limestone comprises up to 50% of the total faulted succession. As described later, only at major complexities in the fault structure do Lower Coralline fault products contribute a significantly larger proportion of the fault content.

4.2. Globigerina Limestone

Globigerina Limestone is preserved in the fault zone as intensely deformed sheets that directly overlie the Lower Coralline Limestone. Owing to its high porosity and low intergranular strength, the Globigerina Limestone has predominantly fragmented by the development of a network of deformation bands associated with localised granulation and grain comminution. This has resulted in fault breccias

containing sub-rounded clasts up to 20 cm long within a fine-grained matrix of granulated Globigerina Limestone (Fig. 9a).

Fault rock derived from the Globigerina Limestone is generally preserved in lensoid pods, restricted to the furrows of the corrugated footwall slip surface (Fig. 9b). Where measurable, the corrugations have strike-parallel lengths of 2 to >10 m and amplitudes of up to 3 m. We interpret the corrugations to result from the displacement of Lower Coralline Limestone lenses, which were incorporated within the fault zone by the coalescence of overlapping footwall slip surfaces or by shearing off of asperities from the footwall (Childs et al., 1996a,b; Ferrill et al., 1999). Outside of the corrugations, Globigerina Limestone fault rock is scarce, probably because it is friable material and was easily removed by the subsequent displacement of the Blue Clay and Upper Coralline Limestone down the fault. For this reason the Globigerina Limestone fault rocks are distributed erratically along the fault, as shown in Figs. 5c and 6.

4.3. Blue Clay

The Blue Clay Formation represents 40–86% of the exposed fault zone within the central part of the Maghlaq Fault trace between Ras Hanzir and Ras il-Hamrija (Fig. 5a; sections

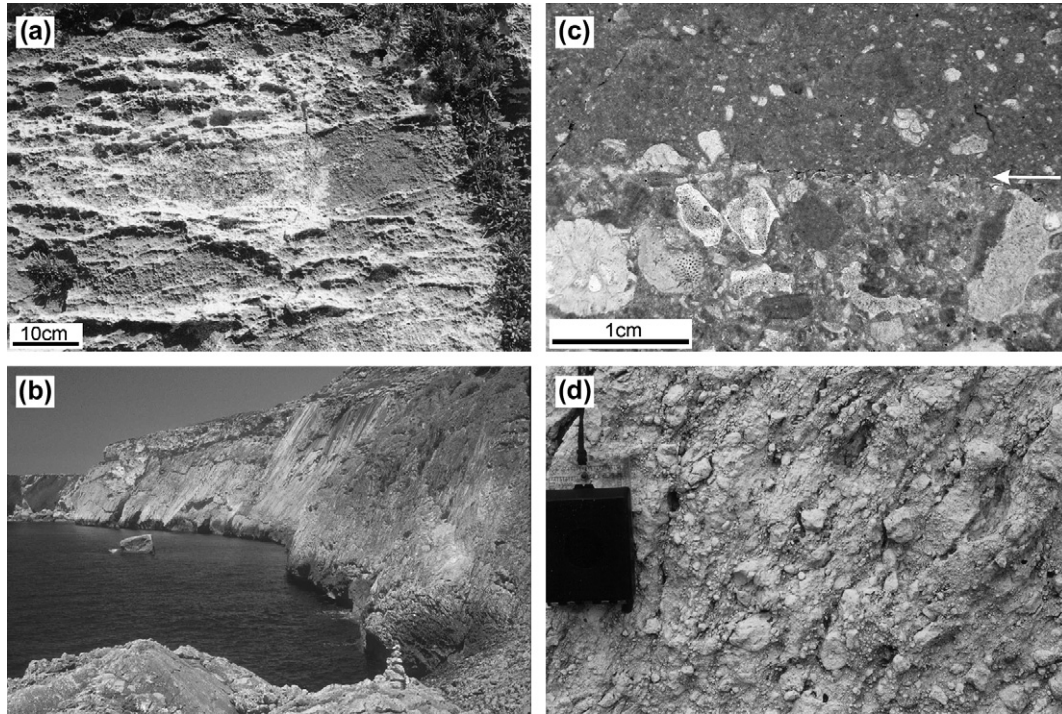


Fig. 7. Faulted Lower Coralline Limestone. (a) Fault-related deformation bands in the footwall at Ras il-Hamrija (see Fig. 4 for location). The shears are more resistant than the host Lower Coralline Limestone and therefore weather as prominent ridges. (b) Prominent Lower Coralline Limestone fault surfaces of the Maghlaq Fault which constitute resilient sea cliffs between Tal-Gawwija and Ras il-Hamrija (see Fig. 4). Cliff height is 30–40 m. (c) Photomicrograph of the sharp boundary (arrow) between fine grained, cataclastically deformed Lower Coralline Limestone fault rock and the relatively undeformed protolith. (d) Highly porous Lower Coralline Limestone breccia comprising coarse angular fragments. The compass-clinometer is 10 cm long.

D–D', E–E', F–F' and G–G'). It reaches a maximum thickness of 22.5 m at Ras Hanzir, where the basal contact of the Blue Clay with the underlying Globigerina Limestone can be seen within the fault zone (Fig. 5a; section D–D'). The Blue Clay is relatively undeformed in these areas, but green-blue depositional laminations in the sediment are locally rotated up to 30° towards the hangingwall of the fault, as at Ras Hanzir and Ras il-Hamrija. Despite the large thickness of Blue Clay within the fault zone in the eastern exposures, the exposed thickness of Blue Clay along the western extent of the fault is <1 m, such that no clay occurs within the fault zone at Ix-Xaqqa (Fig. 5a; section A–A'); although a data gap of 0.75 m exists within this section, it occurs stratigraphically below the Blue Clay. In the absence of reverse movement within the fault zone, for which there is no evidence, the gap must represent eroded Globigerina Limestone. The extreme variability in clay thickness, represented schematically in Fig. 6, is best seen at Ras Hanzir (Fig. 5a). Here, the Blue Clay thickness varies from 0–22.5 m over a 170 m strike length of the fault (Fig. 5a; sections B–B', C–C' and D–D'). Relative to the predicted thickness, T_{LITH} , the Blue Clay is over-represented in the fault zone by a factor of 2–4 times, but where the fault zone is narrow the Blue Clay is absent.

4.4. Upper Coralline Limestone

The Upper Coralline Limestone sediments provide a continuous fault rock component along the length of the fault

(Fig. 5c). They comprise a highly sheared belt, 2–10 m wide, which is intensely foliated and separated from the less-deformed hangingwall by a discrete shear surface, or by a high strain zone (<0.5 m wide) where the hangingwall beds are dragged and attenuated into parallelism with the fault (Fig. 6). Scarce remnants of the Greensand Formation outcrop sporadically as a discontinuous layer along this contact, rotated parallel to the fault zone (Fig. 5a, section F–F').

5. Fault zone complexities

The Maghlaq Fault is a relatively simple structure over most of its length, comprising two principal slip surfaces that bound deformed rocks arranged in stratigraphic order from footwall to hangingwall. Areas of more complex geometry are located at branch-lines and at bends in the trace of the fault. These are interpreted to be sites of linkage of fault segments that were initially arranged in an échelon geometry. Below we present descriptions of a breached relay zone, branch-lines and mature fault bends which give rise to anomalous areas of complex fault zone structure along the Maghlaq Fault. Although similar complexities exist on normal faults of all sizes, their detailed characteristics are rarely described. The superb exposure afforded by the coastal outcrops along the length of the Maghlaq Fault allow for both the analysis of fault zone structure and the interpretation of processes associated with its evolution.

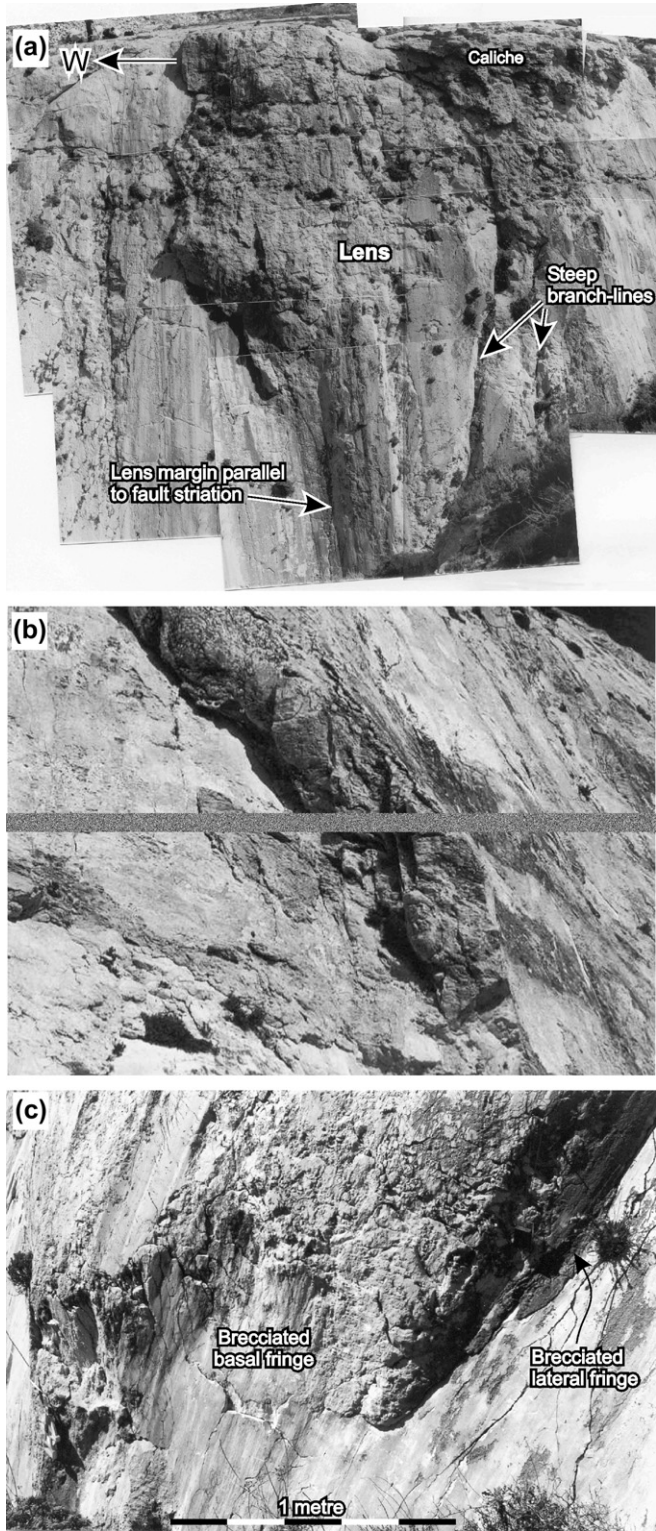


Fig. 8. Lower Coralline Limestone lenses within the Maghlaq Fault zone. (a) Photo-montage of lens formed by coalescence of overlapping slip surfaces at Ix-Xaqqa. The lens is elongate down dip and is bound by steeply plunging branch-lines of similar orientation to the slip striations. The height of the outcrop is approximately 25 m. (b) Oblique view of a lens margin at Ras Hanzir. Riedel shears cut through the lens causing thinning and elongation. Lens thickness is approximately 60 cm. (c) Tapering basal and lateral fringes of a lens at Ras Hanzir (lens 7 on Fig. 14a and c). Both margins comprise cohesive fault breccia, but the lens core is relatively intact. Note the similarity in orientation of the lateral margins of the lens with the fault striations.

5.1. Breached relay zone

At Tal-Gawwija (Fig. 4), part of a highly deformed rock volume between two overlapping fault segments of the Maghlaq Fault is exposed at the level of the basal contact of the Globigerina Limestone with the Lower Coralline Limestone (Fig. 10). The faults have a perpendicular separation of approximately 50 m, between which the upper contact of the Lower Coralline Limestone defines a gently west-southwest dipping ramp. Although displacement variations on the hangingwall ramp-bounding fault cannot be demonstrated, the footwall fault displacement diminishes from about 30 m, at the western edge of the relay ramp outcrop, to 7 m approximately 180 m to the ESE. These observations and the highly faulted

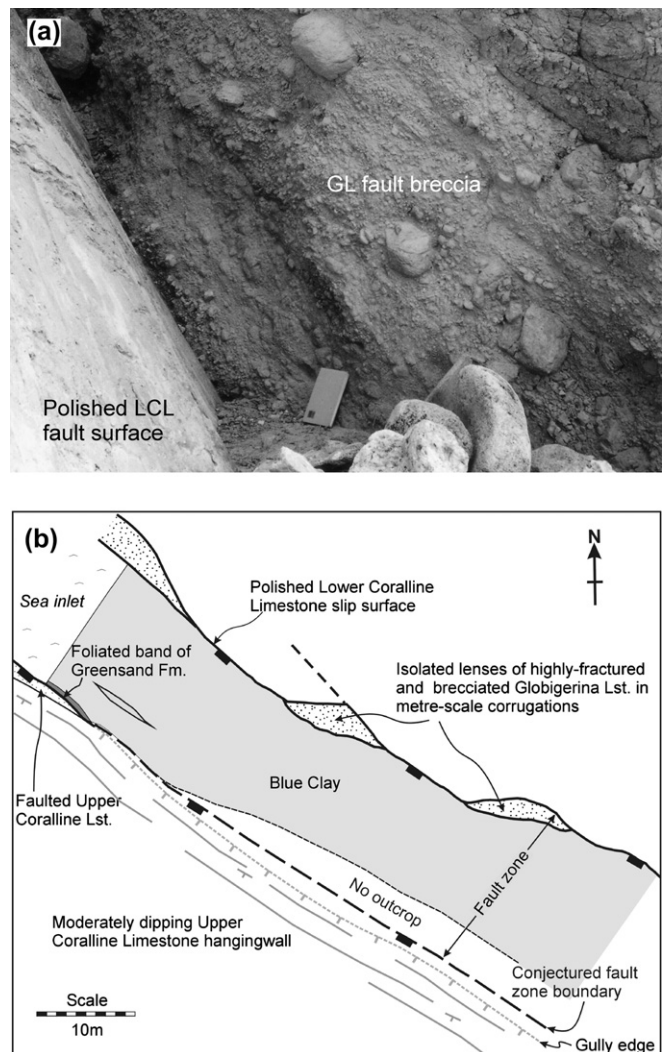
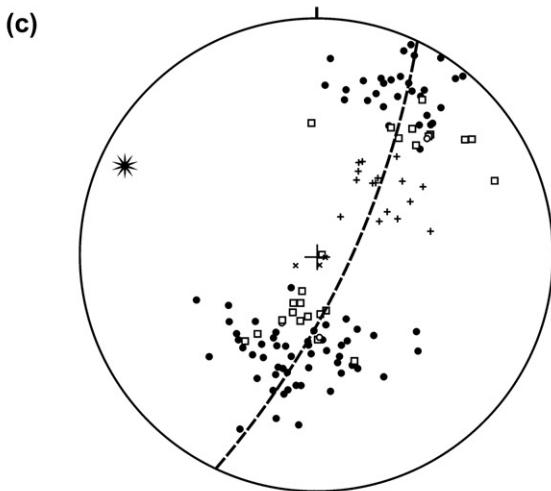
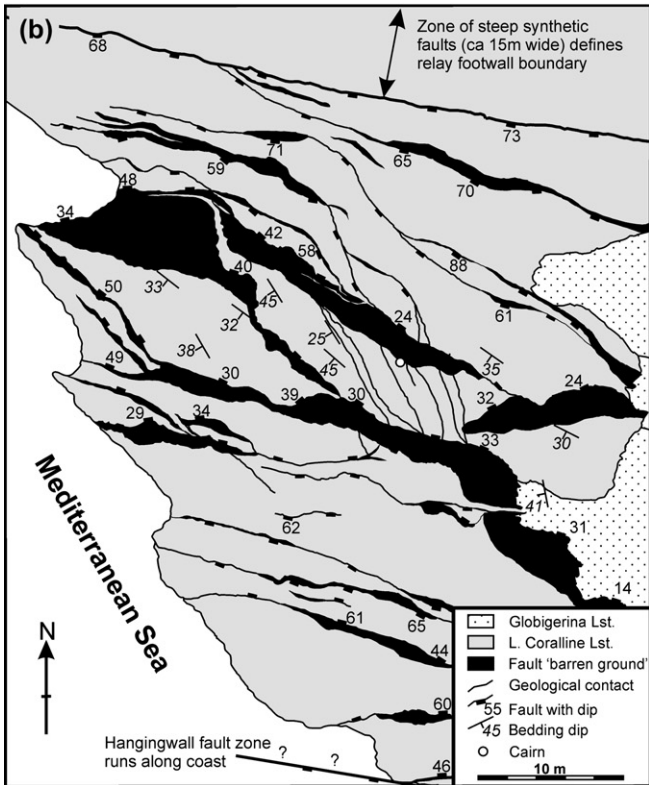
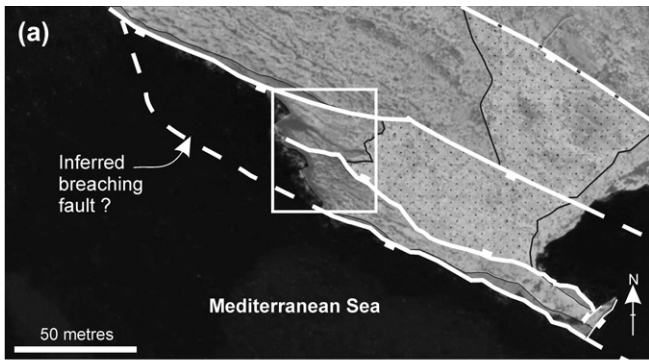


Fig. 9. Faulted Globigerina Limestone. (a) Highly disaggregated Globigerina Limestone breccia juxtaposed against polished Lower Coralline Limestone slip surface at Ras Hanzir (Fig. 4). Approaching the slip surface the fault rock grades from a jigsaw breccia (top right) to a coarse breccia of sub-rounded cm-scale clasts in a moderately cohesive fine-grained matrix. The notebook is 20 cm long. (b) Map of the fault zone exposed in the Il-Miqtub sea inlet (Fig. 4), illustrating the occurrence of the Globigerina Limestone within the fault zone as discontinuous lenses, commonly restricted to concave corrugations on the footwall slip surface.



- Pole to fault
- Slickenline
- + Pole to bedding within relay
- × Pole to bedding outwith relay
- Best-fit great circle (faults & bedding)
- * Pole to great circle

nature of the ramp support our interpretation that the structure represents a highly deformed relay ramp, that is most probably breached off-shore (Fig. 10a; Peacock and Sanderson, 1994; Childs et al., 1995; Walsh et al., 1999).

The gross strike and dip of the relay ramp is broadly 170/07 WSW, defined by a best-fit surface of the Lower Coralline Limestone upper contact. Locally the Lower Coralline Limestone contact dips 15–45° SSW within decimetre-scale blocks bound by minor synthetic and antithetic faults within the relay ramp (Fig. 10b). The synthetic faults are common along the margins of the relay ramp and dip 53–89° SSW (average = 68°). In contrast, the antithetic faults dip 14–69° NNE (average = 39°) and are particularly well-developed within the centre of the relay ramp, where they comprise a hard-linked network (Fig. 10b). Synthetic faults accommodate near-pure dip-slip displacements (average lineation azimuth = 199°), whilst the antithetic faults consistently have a right-lateral slip component, on average trending 22.5° clockwise of the fault dip (average lineation azimuth = 043°). Antithetic faults account for approximately 70% of the extension accommodated in the ramp, and the maximum observed displacement of 5 m is associated with an antithetic fault. A single cross-cutting relationship has been observed, where an antithetic fault with 5 m displacement is offset 0.5 m by a synthetic fault.

Synthetic ramp faults have similar dips to the ramp bounding faults and to synthetic faults outside the relay ramp. We suggest, therefore, that the synthetic faults have not rotated significantly as their dips are similar to the bulk shear plane of the fault zone. Poles to the synthetic and antithetic fault sets are asymmetrically distributed about the poles to bedding within the relay ramp (Fig. 10c). However, when layering within the rotated block is restored to horizontal and the antithetic faults are rotated by the same transformation, the two fault sets are broadly symmetrically distributed about the poles to bedding. This indicates that the antithetic faults initiated as moderately dipping structures (average restored dip = 64°) and were subsequently passively rotated to shallower angles between the synthetic ramp faults. Oblique slip on the antithetic faults account for the fault parallel components of relay ramp dip.

In the proximity of the Tal-Gawwija relay ramp, bedding surfaces are present in the Lower Coralline Limestone, but have vertical spacings of 2–15 m. Unlike relay ramps in strongly anisotropic multilayered rocks, where ramp rotation can be accommodated to a large extent by flexural slip along

Fig. 10. (a) Interpreted aerial photograph of the Tal-Gawwija breached relay ramp. The boxed area denotes the position of b. The trace of the inferred breaching fault offshore is unknown. (b) Baseline grid map of the breached relay (boxed area in a). Relay deformation is accommodated by a network of synthetic and antithetic faults that cause locally high bed dips. Towards the S of the exposure, solution erosion is intense and the relay deformation is mapped in less detail. (Cairn is located at E0449713 N3964397). (c) Equal area stereonet of structural data from the relay ramp. The pole to the fitted great circle represents the common intersection point of intra-relay faults (synthetic and antithetic), relay bedding and ramp-bounding faults.

layering (Walsh et al., 1999), relay ramps in relatively massive successions must achieve a coherent deformation primarily through slip on different fault sets. The highly faulted nature of the relay ramp is consistent with data from other faults in Malta indicating that, relative to their displacements, fault frequencies (faults m^{-1}) within breached relay ramps can be 1–2 orders of magnitude greater than elsewhere along the lengths of individual faults. The average common intersection orientation between the intra-relay faults (synthetic and antithetic), relay ramp bedding and ramp-bounding faults is 11/295 (Fig. 10c). This geometrical configuration provides a coherent means of ramp deformation by the intersection of opposed-dipping (synthetic/antithetic) fault sets within the plane of bedding-parallel slip surfaces. The precise details of the deformation are complex, but the overall WSW ramp dip is likely to result from a combination of fault-parallel rotations, which accommodate displacement transfer between fault segments, and local block rotations resulting from normal-oblique-dextral slip on the antithetic faults.

5.2. Branch-lines

Following the usage of Boyer and Elliot (1982), we refer to a branch-line as the line of intersection between two segments of a multi-strand fault (see Walsh et al., 1999 for 3-D examples associated with normal faults). The plunge and azimuth of the branch-line depends on the relative orientations of the intersecting faults and may range in attitude from horizontal to a maximum plunge equal to the dip of the steeper fault. With fault exposures up to 40 m high, the study area provides an excellent opportunity to examine several steep to sub-vertical plunging branch-lines. Here we describe the architecture of two examples.

5.2.1. Branch-line at Ras il-Hamrija

Between Halq it-Tafal and Denb il-Baghal, the Maghlaq Fault comprises two principal fault traces, with a maximum separation of ca 100 m (Fig. 4). At the Ras il-Hamrija sea inlet, the 20 m wide fault zone of the southernmost of the two principal fault traces is intersected by a minor, east-northeasterly trending fault (throw = 9–25 m), which links to the northernmost principal fault trace (Figs. 4 and 11a). The minimum estimate of displacement on the northern and southern principal traces of the Maghlaq Fault are approximately 37 m and 105 m, respectively. The linking fault is tentatively interpreted as an abandoned relay-breaching fault (Peacock and Sanderson, 1994; Childs et al., 1995; Walsh et al., 1999); the relay zone was finally breached along a fault 120 m to the east–southeast of the branch-line, now seen as a bend in the fault trace (Fig. 11a).

The branch-line between the linking fault and the southern fault trace is well exposed in 25 m high cliffs, where the cliff surface is the footwall surface of the southern principal fault (Fig. 11a and b). The principal footwall fault surface has been downthrown to the SE by the intersecting minor fault, giving a plan view offset of 4 m (Fig. 11a, inset). By contrast the hangingwall slip surface of the fault zone is not offset,

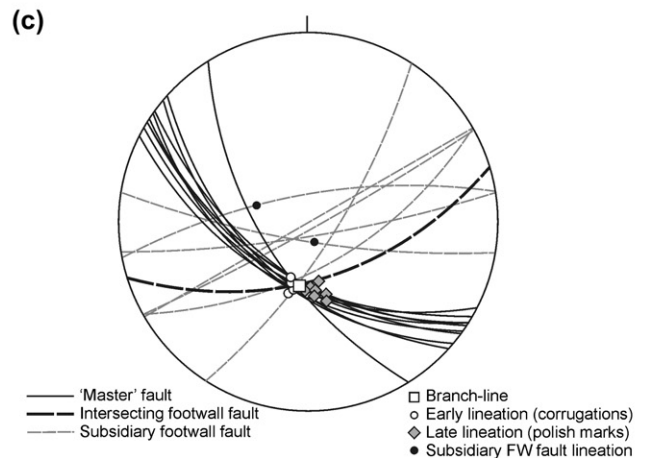
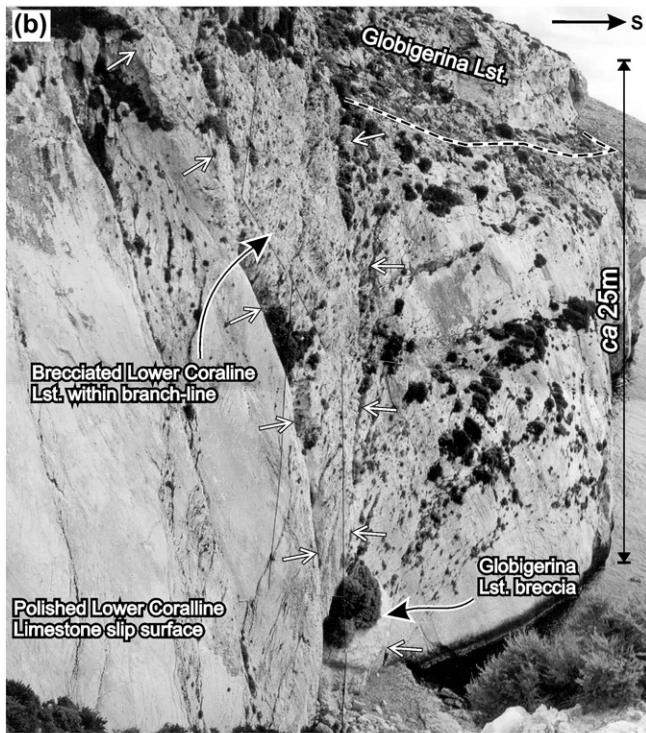
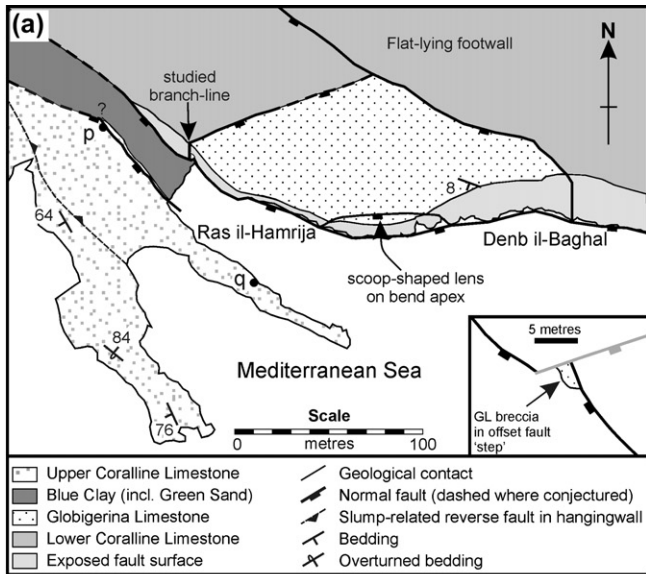
suggesting that it post-dates the formation of the branch-line, or the minor fault terminated within the major fault zone. The step in the footwall fault surface is filled with a moderately plunging (62/189) columnar wedge of coarsely brecciated Lower Coralline Limestone, with a subordinate volume of Globigerina Limestone breccia near the base (Fig. 11b). Near the top of the cliff, where erosion is subdued, a wedge of intensely brecciated footwall Lower Coralline Limestone, with a maximum horizontal length of about 8 m, completely in-fills the step within the master fault surface. The breccia comprises angular clasts of Lower Coralline Limestone, 1 mm to 10 cm long, which define a weak shape fabric dipping 55–65° west at the accessible level of the outcrop. Although the breccia is cohesive, it maintains a fracture porosity of up to 5%.

In the proximity of the branch-line, two directions of fault slip occur on the southern principal fault surface. From overprinting relationships, the earlier features are metre-scale wavelength, low amplitude (ca 10 cm) corrugations that pitch around 75–80° ESE (Fig. 11c), oriented sub-parallel to the branch-line. These are post-dated by fine scratch and polish marks that plunge 65–70° ESE. Although striations were not observed on the main intersecting fault, lineations on footwall splays to this fault indicate pure dip-slip to oblique WSW movement (Fig. 11c), accounting for the lateral offset of the principal fault across the branch-line. A minimum throw of 8.6 m on the intersecting fault is necessary to obtain the observed 4 m lateral offset of the principal fault, assuming a pure dip-slip displacement.

5.2.2. Branch-line at Halq it-Tafal

A complex branch-line is exposed in the footwall of the main Maghlaq Fault surface in sea-cliff exposures, reaching nearly 30 m high, at Halq it-Tafal (Figs. 4 and 12a). The main east-southeast trending (118° strike) Maghlaq Fault is intersected at a very acute angle (9°) by a footwall fault (109° strike) (Fig. 12a). Throws on the footwall and hangingwall faults are 65–90 m and >129 m, respectively.

Unlike the previous example, the intersection line of the two fault planes cannot be observed at Halq it-Tafal. Instead, the branch-line is marked by extensive brecciation (minimum thickness = 5 m), extending along strike of the fault zone for 90 m (Fig. 12a and b). Poor outcrops preclude delineation of the complete extent of the breccia into the footwall. However, given the intensity of the deformation, we conjecture that brecciation occurs throughout a triangular wedge within the apex of the intersecting faults. To the west, the breccia sheet pinches out to reveal a smooth fault surface of the western fault plane (Fig. 12a). To the east, the breccia ends abruptly, in a series of sheets that inter-finger with intensely fractured Lower Coralline Limestone. As the branch-line is approached from the ESE, the dip of the Lower Coralline Limestone increases from sub-horizontal to 24° WNW (Fig. 12b) and is increasingly disrupted by synthetic and antithetic faults with centimetre to metre-scale throws, reflecting the high strain at the branch-line.



Fault breccia associated with the branch-line is cohesive and contains angular to moderately rounded clasts, with diameters of a few mm to several cm. Pore spaces within the breccia are not occluded by cements, so that high porosities are preserved. The breccia is overprinted by a weak fabric defined by minor slip surfaces and a spaced fracture foliation subparallel to the footwall fault (Fig. 12c). Additionally, a narrow east–southeasterly dipping fault zone cutting across the centre of the wedge reworks and displaces the breccia by about 3 m (Fig. 12b and c), accommodating localised slip sub-parallel to the branch-line.

Two slip directions are present in the vicinity of the Halq it-Tafal branch-line (Fig. 12c). One lineation is defined by subtle corrugations (wavelength = <1 m; amplitude = <0.1 m) and polish marks that plunge steeply to the east (average = 61/201). A second slip direction is defined by gutter marks (Hancock and Barka, 1987), fine striations and polish marks that plunge less steeply towards the east (average = 56/181). Cross-cutting relationships can be observed immediately west of the breccia wedge, indicating that the shallower lineation is younger. This lineation overprints the breccia wedge, indicating that it post-dates fault linkage (Fig. 12b).

5.2.3. Branch-line kinematics

Cross-cutting fault striations on the Maghlaq Fault have only been observed within approximately 100 m of the two major branch-lines, described above. We suggest that the presence of two sets of striations indicates a change in the local fault kinematics during the formation and subsequent modification of the branch-line. In the Ras il-Hamrija example, the coincidence between the branch-line orientation and that of the earliest preserved slip lineation on the principal fault (Fig. 11c) is interpreted to indicate that the branch-line kinematically constrained the fault slip direction, albeit transiently. Later fault striations that plunge more shallowly than the branch-line probably reflect a return to the far-field slip direction, as the influence of the branch-line became subdued by fault zone processes and/or by the abandonment of the branch-line.

The occurrence of two slip orientations and their cross-cutting relationships in the vicinity of the Halq it-Tafal branch-line (Fig. 12c) is remarkably similar to the Ras il-Hamrija example (Fig. 11c) and also lends itself to an interpretation in which the earlier lineation is kinematically controlled

Fig. 11. (a) Geological map of the studied Ras il-Hamrija branch-line. Point 'p' denotes the position of the viewpoint for Fig. 11b, whilst Point 'q' shows the viewpoint for Fig. 15. The hangingwall structure is supplemented with data from Dart (1991). Inset: sketch map enlargement of the offset trace of the principal fault. (b) Photo-montage of the branch-line intersection with the polished main footwall slip surface of the Maghlaq Fault, exposed as southwesterly facing cliff, viewed towards the ESE. The fault intersection is marked by a steeply inclined zone of coarsely brecciated Lower Coralline Limestone (highlighted by arrows) and, at the base of the outcrop, Globigerina Limestone breccia. (c) Equal area stereonet of fault data derived from the branch-line area. Note the close coincidence between fault slip lineations on the 'master' fault and the branch-line orientation.

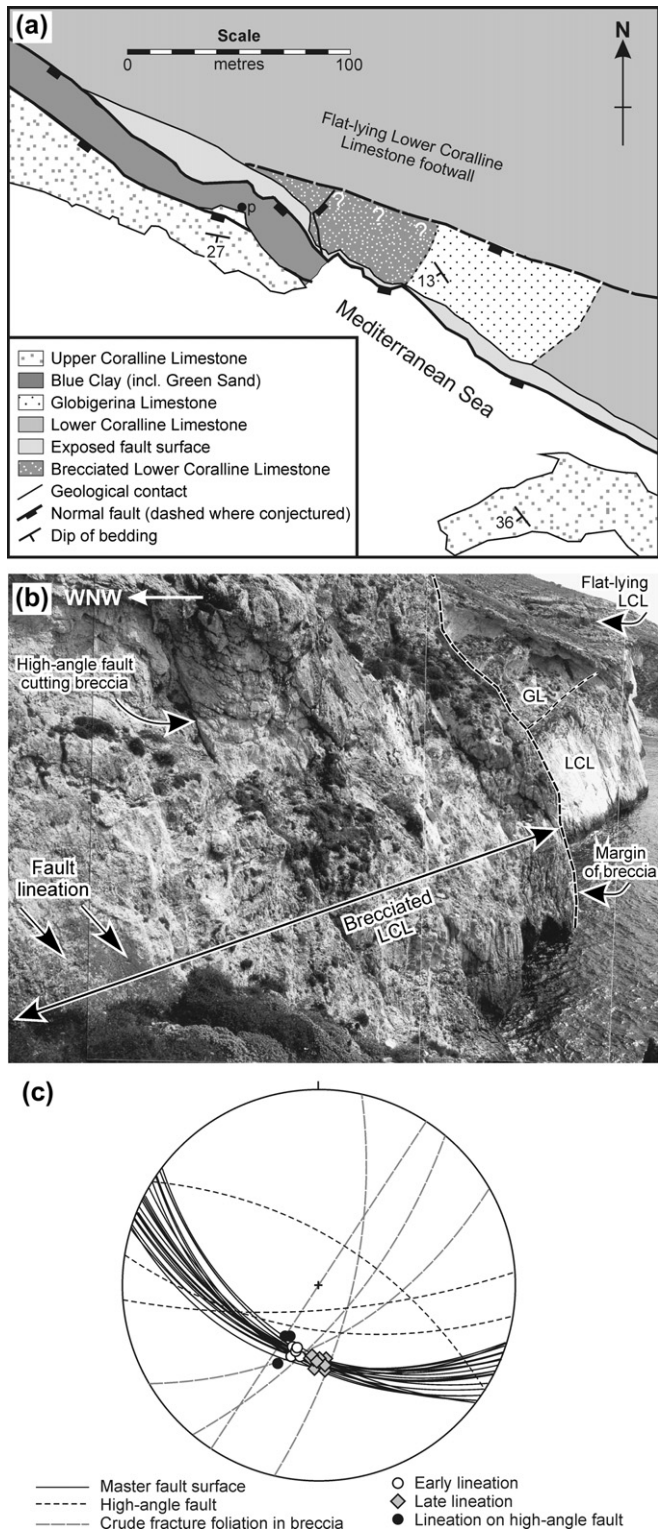


Fig. 12. (a) Geological map of the branch-line outcropping at Halq it-Tafal. Point 'p' denotes the viewpoint of b. (b) View looking ESE along the brecciated Lower Coralline Limestone at the apex of the branch-line. Immediately beyond the breccia, the contact of the Lower Coralline Limestone with the Globigerina Limestone is dragged towards the branch-line apex. In the distance the Lower Coralline Limestone beds are flat-lying. The cliff height in the foreground is approximately 30 m. (c) Equal area stereonet of fault data derived from the branch-line area.

by the branch-line and the later lineation reflects a return to the regional slip direction. The earliest slip lineation preserved would, in this interpretation, reflect the average branch-line orientation between the hangingwall fault (mean orientation = $118/60$ SSW) and the footwall fault, which strikes 109° . The dip of the latter is unknown, but for our interpretation to be correct could range between 56° and 62° , close to the modal fault dip value of 60° measured along the Maghlaq Fault.

When faults of different orientation coalesce, the initial branch-line becomes the axis of a bend on the modified normal fault surface (Fig. 13a). The range of possible angular bend/branch-line orientations is a function of the relative attitudes of the two intersecting faults (Fig. 13) and may range from horizontal, resulting from two parallel but unequally dipping faults, to steep, where the plunge is only limited by the dip of the steeper intersecting fault. In the case of faults with relatively steep dips, the branch-line may plunge towards or away from the direction of fault convergence (Fig. 13a and c). Given the large range of possible branch-line orientations that could occur (Fig. 13c), the fact that the Ras il-Hamrija and Halq it-Tafal examples are oriented sub-parallel to the approximately N–S (007°) far-field slip direction of the Maghlaq Fault (Dart et al., 1993) suggests that they form in relatively stable kinematic configurations. Other minor branch-lines at Ix-Xaqqa (Fig. 4) are oriented parallel or sub-parallel to the far-field slip direction, as are fault zone lens margins (Fig. 8) and fault surface corrugations (e.g. Il-Miqtub; Fig. 9).

The presence of a sharp bend on a fault surface at a branch-line represents a physical obstacle to fault slip in directions other than parallel to the bend axis and, if large enough, may cause fault slip to re-orient parallel to it, at least temporarily. Strain compatibility problems (e.g. dilation and volume loss) about the angular bend at the branch-line intersection would be minimal if the slip direction parallels the bend axis. However, a bend oblique to the slip direction of the fault would represent either an asperity to slip or a dilational bend. With increasing displacement, these are likely to succumb to mechanical erosion, or would be in-filled by fault products, allowing the fault slip direction to return to the far-field slip direction. Despite the small mismatch between the branch-line orientations and the far-field slip direction at the two large branch-lines described ($5\text{--}10^\circ$), significant strain compatibility problems occurred as evidenced by the large breccia volumes generated adjacent to each.

5.3. Fault bends

Distinct bends in the trace of the mainly ESE striking Maghlaq Fault are defined by E–W striking portions, such as at Ras Hanzir and Ras il-Hamrija (Fig. 4), which together define a left-stepping fault trace. The shorter, more E–W striking portions are interpreted as breaching faults arising from the growth and failure of relay ramps between left-stepping fault segments (Childs et al., 1995; Ferrill et al., 1999). Bends along the Maghlaq Fault are therefore interpreted as examples of long-established points of segment

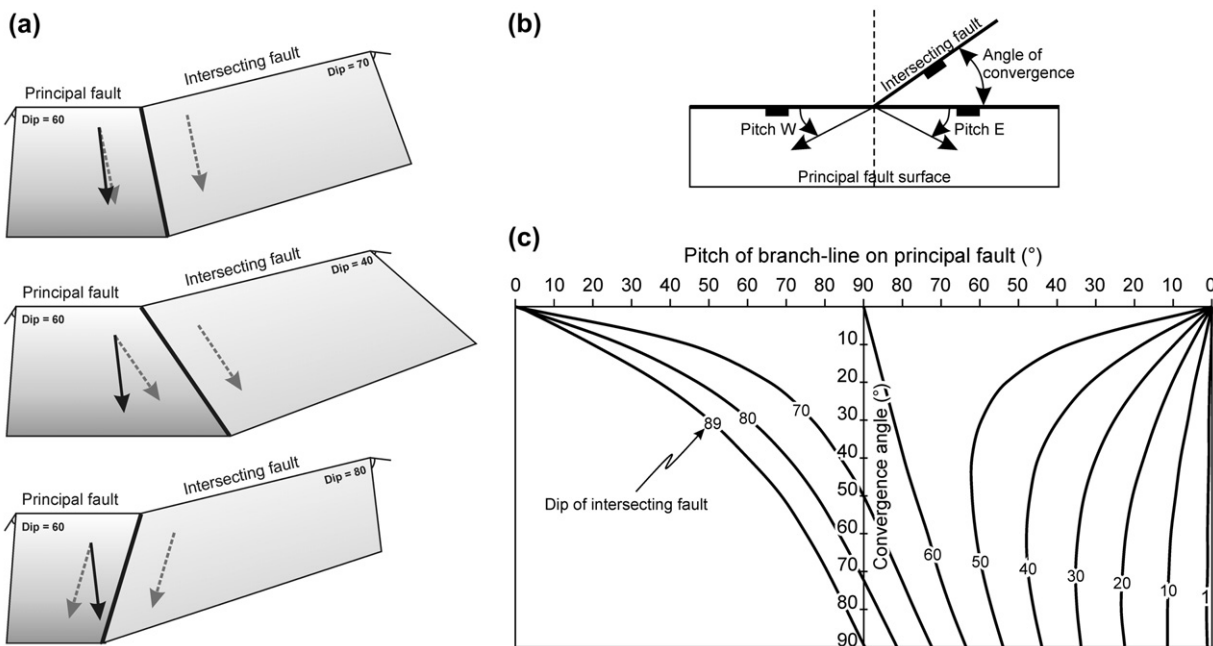


Fig. 13. (a) Schematic diagrams illustrating the variability in branch-line orientations between a 60° dipping principal fault and an intersecting fault with dips of 60°, 40° and 80°. Black arrows represent the far-field extension direction. Dashed grey arrows represent branch-line parallel slip, i.e. slip which minimizes related strain compatibility problems. (b) Scheme of measurements used on plot c. (c) Plot showing the variation in branch-line pitch on a 60° dipping principal fault for varying intersection angles of footwall intersecting faults that range in dip from 1° to 89° (labelled curves). For intersecting faults steeper than the principal fault, the angle of intersection may plunge in the direction of fault trace convergence. Intersecting faults dipping less than the principal fault always plunge away from the direction of fault trace convergence.

linkage. It follows that the fault bends represent mature branch-lines.

5.3.1. Fault bend at Ras Hanzir

At Ras Hanzir, the trace of the footwall slip surface changes in strike from approximately 100° to 060° over 200 m, defining a sharp footwall bend (Fig. 14a). Between the apex of the bend and about 100 m to the east, are a series of lens-shaped lozenges of Lower Coralline Limestone (Fig. 14c). These range in scale from metres to decametres: the larger lenses measure 30–50 m parallel to the fault strike, are up to 5 m thick and, prior to erosion, would have exceeded the vertical height of the cliff exposures (>35 m) (Fig. 14c). These E–W striking lenses overlap in a left-stepping sense about the western part of the bend (Fig. 14a). The apparent flat-topped nature of the lenses is interpreted as the contact of the Lower Coralline Limestone with the less resistant (now eroded) Globigerina Limestone. A decrease in the elevation of these flat tops towards the apex of the bend (i.e. southwesterly) therefore reflects an increase in the displacement of the lenses. A lens of highly deformed Globigerina Limestone on the bend apex represents the furthest travelled lens (lens 1 in Fig. 14a and c). The fault trace defined by the hangingwall of the lenses is more smoothly curved than that of the footwall (Fig. 14a), indicating that the angularity of the fault has been decreased by the mechanical erosion of the footwall limestones into lenses and by their subsequent internal deformation and translation in the fault zone. The poles to the curved footwall fault surface at Ras Hanzir plot as a great circle on a stereonet, oriented

090/19N (Fig. 14c), indicating that the fault bend approximates a cylindrically curved surface (Fig. 14b). A near-constant slip azimuth about the bend of 70/180 is achieved by a systematic change in the lineation pitch, from 71° E in the west, to 67° W in the east. This slip direction is very similar to the 007° far-field extension direction determined by Dart et al. (1993). The development of the cylindrical fault bend axis in the orientation of the regional slip direction maintains strain compatibility while reducing surface irregularity, hence frictional resistance to fault slip.

5.3.2. Fault bend at Ras il-Hamrija

A similar, but less accessible, example of a fault bend outcrops in the sea cliffs approximately 100 m east of Ras il-Hamrija (Figs. 4 and 11a). Here the main trace of the Maghlaq Fault changes in strike from approximately 130° to 80°. A decametre-scale scoop-shaped lens, derived from the footwall Lower Coralline Limestone and Globigerina Limestones, occupies the apex of the bend (Fig. 15). The lens is approximately 65 m wide, 20 m thick and >35 m high and has been displaced vertically 8–10 m along the footwall slip surface. The lens appears to have undergone some rotation in sympathy with the fault displacement, indicated by the 30–40° S dip of the Lower Coralline contact with the Globigerina Limestone, revealed by partial erosion of the less resistant, younger limestone. However, deformation of the lens appears less intense than at Ras Hanzir, with only one other lens being partially exposed lower down in the cliff face (Fig. 15).

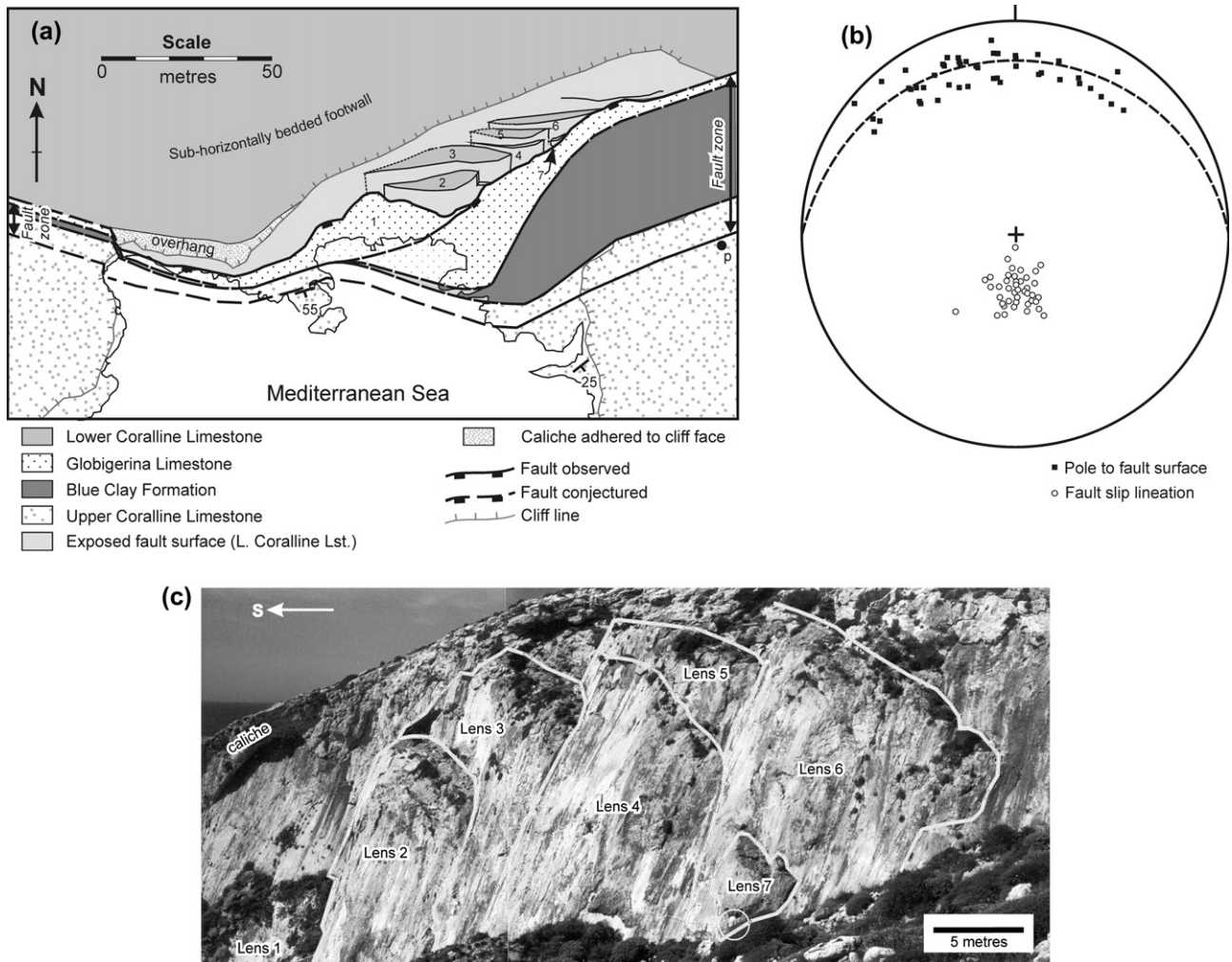


Fig. 14. (a) Geological map of the Ras Hanzir fault bend, illustrating the rapid changes in fault zone thickness from west to east and the development of a series of stacked lenses, annotated 1 to 7. (Point 'p' denotes the position of the viewpoint of c.) (b) Stereonet of fault data derived from the footwall slip surface of the fault bend. (c) View of the overlapping lenses on the footwall slip surface, looking WNW. Fault zone lenses are annotated 1 to 7 as in a. Note the person for scale (circled).

6. Discussion

This discussion considers three main questions. What were the fundamental controls on the development of the structure and content of the Maghlaq Fault zone during its growth? How does the Maghlaq Fault zone differ from other faults and what factors are responsible for these differences? Finally, how might the heterogeneous nature of the structure and content of fault zones, as observed in the Maghlaq Fault, influence fluid flow in similar fault systems?

6.1. Development of the Maghlaq Fault zone

The absence of faults of similar orientation and size close to the Maghlaq Fault suggest that its individual segments formed as elements of a coherent fault array (Walsh et al., 2003). The systematic arrangement of the segments as a left-stepping array suggests an underlying basement control on their locations. We suggest that the Maghlaq Fault formed by upward propagation during early extension, associated with the

development of the Pantelleria Rift during Burdigalian times (Dart et al., 1993).

The breached relay, branch-lines and bends documented here illustrate progressive stages of linkage between the individual strands of a segmented normal fault (e.g. Peacock and Sanderson, 1991, 1994; Childs et al., 1995, 1996a; Ferrill et al., 1999; Walsh et al., 1999, 2003) and most of the structural complexities of the Maghlaq Fault can be explained in these terms. Elevated strains occur within relay zones to accommodate ramp rotation (e.g. the relay ramp at Tal-Gawwija). Eventually strain within the relay zone can no longer be accommodated by ramp deformation and the relay zone becomes breached by linkage between the two bounding faults to form a through-going fault (Peacock and Sanderson, 1991; Childs et al., 1995). The site of the former relay zone is preserved as a bend or dog-leg on the trace of the new continuous fault (e.g. Ras Hanzir and Ras il-Hamrija). The axis of the bend in the fault surface is unlikely to be oriented exactly parallel to the overall fault slip vector and the bend will therefore remain a focus for high strain. This fault surface irregularity

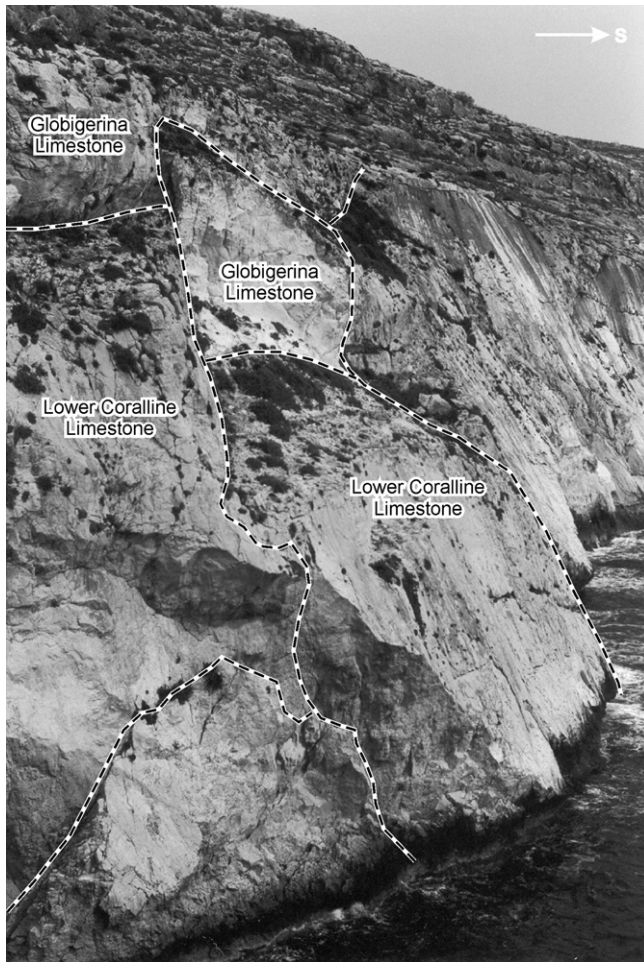


Fig. 15. Photograph of a large scoop-shaped lens on the bend apex at Ras il-Hamrija, looking WNW (viewpoint is shown in Fig. 11a; point 'q'). The lens measures about 65 m wide, 20 m thick and >35 m high, and has been displaced vertically 8–10 m along the footwall slip surface. Cliff height is approximately 35 m.

can be removed by minor modification of the active slip surface, as for example the footwall of the fault bend at Ras Hanzir, or by creation of a new linking fault to form a fault bounded lens, as in the case of Ras il-Hamrija.

Progressive breaching of relay ramps, straightening of fault bends and removal of fault irregularities gives rise to complex and anomalously wide fault zones. These processes reduce the overall active trace length of the fault and smooth fault surfaces. These modifications both reduce the frictional resistance to slip on the fault surface and the requirement for volumetric strains associated with fault sidewall incompatibility.

There are no intact relay ramps along the exposed trace of the Maghlaq Fault but fault bends representing the sites of large scale relay zones (100 m separation) are still apparent. There is however an absence of distinct fault segments spaced <50 m. While it might be possible that segmentation did not occur on the smaller scale, we consider it far more likely that segment boundaries with low separations were consumed into the fault zone at displacements significantly lower than that at the present day. The many lenses that occur within

the fault zone (e.g. Fig. 8) represent possible sites of former segment boundaries on all scales below 50 m. There are few means of establishing whether a lens within a fault zone formed by breaching of a segment boundary or by the shearing off of an asperity on an already through-going fault. In certain circumstances it may be possible to differentiate on the basis of structural position, e.g. the lenses on the fault bend at Ras Hanzir probably formed by modification of the footwall of a through-going fault. In most cases the distinction between these two alternatives will be vague in that much fault surface irregularity will be inherited from the initial segmented character of the fault. Once a lens has been incorporated within a fault zone, it may be dissected into smaller lenses by the formation of Riedel shears (Fig. 8b) and the lens margins, effectively branch-lines between slip surfaces, become sites of intense brecciation (Fig. 8c).

We contend that the major structures within the footwall Lower Coralline Limestone exposures developed during the initial 100–160 m of displacement, prior to the juxtaposition of the un lithified hangingwall sediments. The range in these displacements reflects the height of the outcropping fault exposures with respect to the level of the Blue Clay in the hangingwall. We suggest that once the Lower Coralline Limestone was juxtaposed against the Blue Clay and Upper Coralline Limestone, it was energetically preferable for asperities to be accommodated by continuous deformation of the relatively weak hangingwall sediments rather than by the creation of new fractures in the lithified footwall. Therefore, at this time, the footwall deformation would have effectively ceased following segment linkage and lens formation at locations such as the Ras Hanzir bend. Following linkage of the segments, the Blue Clay and Upper Coralline Limestone Formations deformed by macroscopic ductile flow, attenuating into sheets of fault rock.

6.2. Comparison to other fault zones

Some previous studies of faulted carbonate rocks have highlighted the crucial role of pressure solution processes in all aspects of faulting, e.g. fault nucleation (Willemse et al., 1997; Peacock et al., 1998; Graham et al., 2003), the accommodation of volumetric strains (Odonne and Massonnat, 1992), especially displacement gradients around fault tips (Petit and Mattauer, 1995), and the removal of asperities to fault slip (Gratier and Gamond, 1990; Childs et al., 1996a). The absence of features associated with significant pressure solution processes in the Maghlaq Fault zone, at the exposed level, is attributed to the very shallow burial depths at the time of faulting, although we consider it highly likely that these processes played an important role at deeper levels. The lack of pressure solution and the relatively massive nature of the Globigerina Limestone and Lower Coralline Limestone, which diminishes the likelihood of flexural slip, restricts the manner in which strain can be accommodated and favours deformation by small-scale fracture processes. Possible manifestations of this are the extensive deformation band arrays in

more highly strained areas of the footwall and the development of Riedel shears (Fig. 8c) and microfractures within fault lenses. Furthermore, the paucity of vein material and fault rock cements in the Maghlaq Fault zone, contrasts with other faults in limestone where pressure solution processes have been demonstrated to be the predominant source of the vein material (Gratier et al., 1994) and accounts for the highly porous appearance of breccias within branch-lines.

6.3. Implications for fault-related fluid flow

With the exception of the Blue Clay Formation, the faulted strata contain intervals of moderate to highly porous rock. Therefore, neglecting the content of the fault zone, the relative juxtaposition of lithologies other than the Blue Clay would, in general, favour across-fault fluid flow. Only where the Blue Clay is present would the arrangement of wall rocks provide a juxtaposition seal that might retard or prevent across-fault flow (Nybakken, 1991). The Blue Clay is, however, a significant component of the fault zone and its presence along the majority of the exposed fault trace suggests that it forms an extensive and continuous fault rock layer. In sub-surface fluid flow systems the presence of the Blue Clay would be expected to retard flow, either by forming a low permeability barrier to across-fault fluid flow or, in the case of hydrocarbon flow, by defining an impermeable membrane to across-fault flow (due to the typically high entry pressures of clays; Nybakken, 1991; Manzocchi et al., 2002). However in the western end of the fault trace, Ix-Xaqqa and central Ras Hanzir, Blue Clay fault rock is absent. At these localities the fault displacement is about 4 times the clay bed thickness. Clay fault rock continuity data collected from siliciclastic sequences suggests, however, that clay smears are often continuous for displacement:source layer thickness ratios of ~ 7 or less (Lindsay et al., 1993; Yielding, 2002). The reason for the local absence of Blue Clay at relatively low displacement:thickness ratios (~ 7) is not understood, but it may arise from local geometrical effects of the fault, from issues relating to the rheological properties of the faulted sequence or the deformation conditions associated with faulting.

At depths below the level of the Blue Clay in the hanging-wall, the content of the fault zone must comprise fault products derived from the Lower Coralline Limestone, with or without Globigerina Limestone. The Globigerina Limestone is highly porous and the Lower Coralline Limestone contains porous intervals, therefore a juxtaposition seal over a significant vertical extent is unlikely. However, fine-grained cataclasites that coat the polished principal slip surfaces within the Lower Coralline Limestone-derived fault products (Fig. 7b and c) have extremely low porosities and, we presume, low permeabilities. Their low permeability combined with their relatively continuous distribution over the fault surface provides some potential for a decrease in across-fault flow.

The presence of internally fractured lensoid volumes of Lower Coralline Limestone and Globigerina Limestone within the fault zone suggests potential for along-fault fluid flow

particularly around the fractured and brecciated fringes of lenses. Our limited data from the Maghlaq Fault and elsewhere in Malta suggests that the lenses tend to have long axes parallel to their dip direction, with their intersections parallel to the slip direction, imparting a strong up-fault fracture anisotropy.

The potentially most significant areas for fluid flow within the fault zone are the sites of fault segment linkage (breached relays, branch-lines and bends), which correspond to areas with the largest thicknesses of fractured rock. In three dimensions, the linkage structures can extend vertically to a branch-point, or sub-horizontal branch-line where the fault tip-line originally bifurcates (Childs et al., 1995; Huggins et al., 1995; Ferrill et al., 1999; Walsh et al., 1999). It follows that they can represent 1-dimensional conduits of considerable vertical extent, oriented broadly parallel to the fault slip direction. These structures therefore have great potential for tapping deep-seated fluid reservoirs. Indeed, localised up-fault flow of hydrothermal ore fluids within breached relay zones and branch-lines is recognised as an important control on the location of carbonate-hosted Zn–Pb(–Ba) deposits in the Irish orefield (Carboni et al., 2003) and are likely to be important elsewhere. Similarly, in hydrocarbon systems, these structures may represent migration fairways, as shown by Garden et al. (2001), but may also correspond to potential leakage points. Recognition of the depth at which the fault initially bifurcates is critical in the assessment of the potential for up-fault fluid flow. In general, the greater the separation of the original fault segments linked by the relay, branch-line or bend, the deeper the tip-line bifurcation point extends.

7. Conclusions

1. The Maghlaq Fault formed within a carbonate succession at shallow burial depths (<250 m). The rocks are not affected by pressure solution and maintain significant fault rock porosity.
2. The large-scale structure of the Maghlaq Fault zone is interpreted to have evolved through linkage of an initially left-stepping, segmented normal fault array. Fault zone heterogeneities demonstrate stages in the breaching of relay zones at fault segment boundaries with increasing displacement.
3. The fault zone comprises lenses of variably deformed rock bound by discrete slip surfaces over a broad range of scales. The lensoid geometry is due to the breaching of relay zones and fault segment linkage, the inclusion of asperities and the development of minor slip surfaces within the fault zone (e.g. Riedel shears).
4. Fault rock distribution varies from Lower Coralline Limestone derived cataclasites, found over the whole fault surface, to localised breccia pods derived from Globigerina Limestone, reflecting differences in the degree of lithification of the wall rock units at the time of faulting.
5. The fault rocks, derived from fully lithified sediments at the time of faulting, comprise fine-grained veneers of cataclasite and coarse, poorly cemented breccias. Breccia development is largely associated with branch-lines between

connecting faults occurring in response to volumetric strains due to non-colinearity of fault branch-lines and slip vectors.

6. Deformation of the Lower Coralline Limestone in the footwall to the fault zone is restricted to locally developed arrays of cataclastic deformation bands. These arrays may reach several metres in width where fault segments overlap.
7. Fault rock distribution suggests that in general the Maghlaq Fault will provide a barrier to across fault flow, but a conduit to fault parallel flow. Up-fault flow is especially likely at areas of fault heterogeneity.

Acknowledgements

The authors gratefully acknowledge ENI Exploration and Production Division (Milan) for funding this research and Janpieter van Dijk for supporting the project throughout. This research was also partly funded by the IRCSET Basic Research Grant Scheme (project code: SC/2002/246). We are indebted to Chris Dart for advice on potential field localities in Malta and the loan of his thesis, and to Martyn Pedley for valuable information on Maltese geology. Finally we thank David Peacock and Nigel Woodcock for their reviews.

References

- Aydin, A., Johnson, A.M., 1978. Development of faults as zones of deformation bands and as slip surfaces in sandstone. *Pure and Applied Geophysics* 116, 931–942.
- Bennett, S.M., 1980. Palaeoenvironmental studies in Maltese mid-Tertiary carbonates. Unpublished PhD thesis, University of London.
- Bosence, D.W.J., Pedley, H.M., 1982. Sedimentology and palaeoecology of a Miocene coralline algal bioherm from the Maltese islands. *Palaeogeography, Palaeoclimatology and Palaeoecology* 38, 9–43.
- Boyer, S.E., Elliot, D., 1982. Thrust systems. *American Association of Petroleum Geologists Bulletin* 66, 1196–1230.
- Carboni, C., Walsh, J.J., Stewart, D.R.A., Güven, J.F., 2003. Timing and geometry of normal faults and associated structures at the Lisheen Zn/Pb deposit – investigating their role in the transport and the trapping of metals. In: Eliopoulos, D.G., et al. (Eds.), *Proceedings of the Seventh Biennial SGA Meeting – Mineral Exploration and Sustainable Development*. Millpress Science Publishers, Rotterdam, pp. 665–668.
- Cello, G., Crisci, G.M., Marabini, S., Tortorici, L., 1985. Transtensive tectonics in the Strait of Sicily: structural and volcanological evidence from the island of Pantelleria. *Tectonics* 4, 311–322.
- Childs, C., Watterson, J., Walsh, J.J., 1995. Fault overlap zones within developing normal fault systems. *Journal of the Geological Society, London* 152, 535–549.
- Childs, C., Nicol, A., Walsh, J.J., Watterson, J., 1996a. Growth of vertically segmented normal faults. *Journal of Structural Geology* 18, 1389–1397.
- Childs, C., Watterson, J., Walsh, J.J., 1996b. A model for the structure and development of fault zones. *Journal of the Geological Society, London* 153, 337–340.
- Dart, C.J., 1991. Carbonate sedimentation and extensional tectonics in the Maltese graben system. Unpublished PhD thesis, University of London.
- Dart, C.J., Bosence, D.W.J., McClay, K.R., 1993. Stratigraphy and structure of the Maltese Islands. *Journal of the Geological Society, London* 150, 1153–1166.
- Finetti, I., 1982. Structure, stratigraphy and evolution of the central Mediterranean. *Bollettino di Geofisica Teorica ed Applicata* 24, 247–312.
- Ferrill, D.A., Stamatakos, J.A., Sims, D., 1999. Normal fault corrugation: implications for growth and seismicity of active normal faults. *Journal of Structural Geology* 21, 1027–1038.
- Garden, I.R., Guscott, S.C., Burley, S.D., Foxford, K.A., Walsh, J.J., Marshall, J., 2001. An exhumed palaeo-hydrocarbon migration fairway in a faulted carrier system, Entrada Sandstone of SE Utah, USA. *Geofluids* 1, 195–213.
- Gawthorpe, R.L., Sharp, I., Underhill, J.R., Gupta, S., 1997. Linked sequence stratigraphic and structural evolution of propagating normal faults. *Geology* 25, 795–798.
- Graham, B., Antonellini, M., Aydin, A., 2003. Formation and growth of normal faults in carbonates within a compressive environment. *Geology* 31, 11–14.
- Gratier, J.P., Gamond, J.F., 1990. Transition between seismic and aseismic deformation in the upper crust. In: Knipe, R.J., Rutter, E.H. (Eds.), *Deformation mechanisms, rheology and tectonics*. Geological Society, London, Special Publications, vol. 54, pp. 461–473.
- Gratier, J.P., Chen, T., Hellmann, R., 1994. Pressure solution as a mechanism for crack sealing around faults. In: Hickman, S.H., Sibson, R.H., Bruhn, R.L. (Eds.), *Mechanical involvement of fluids in faulting*. USGS Open File Report 228, 279–300.
- Hancock, P.L., Barka, A.A., 1987. Kinematic indicators on active normal faults in western Turkey. *Journal of Structural Geology* 9, 573–584.
- Hill, K.C., Hayward, A.B., 1988. Structural constraints on the Tertiary plate tectonic evolution of Italy. *Marine and Petroleum Geology* 5, 2–16.
- Huggins, P., Watterson, J., Walsh, J.J., Childs, C., 1995. Relay zone geometry and displacement transfer between normal faults recorded in coal mine plans. *Journal of Structural Geology* 17, 1741–1755.
- Jongsma, D., vanHinte, J.E., Woodside, J.M., 1985. Geological structure and neotectonics of the north African continental margin south of Sicily. *Marine and Petroleum Geology* 2, 156–177.
- Lindsay, N.G., Murphy, F.C., Walsh, J.J., Watterson, J., 1993. Outcrop studies of shale smears on fault surfaces. In: Flint, S., Bryant, I.D. (Eds.), *The geological modelling of hydrocarbon reservoirs and outcrop analogues*. Special Publication of the International Association of Sedimentologists 15, 113–123.
- Maltman, A., 1994. Deformation structures preserved in rocks. In: Maltman, A. (Ed.), *The geological deformation of sediments*. Chapman and Hall, London, 261–302.
- Manzocchi, T., Heath, A.E., Walsh, J.J., Childs, C., 2002. The representation of two phase fault-rock properties in flow simulation models. *Petroleum Geoscience* 8, 119–132.
- Nybakken, S., 1991. Sealing fault traps—an exploration concept in a mature petroleum province: Tampen Spur, northern North Sea. *First Break* 9, 209–222.
- Odonne, F., Massonnat, G., 1992. Volume loss and deformation around conjugate fractures: comparison between a natural example and analogue experiments. *Journal of Structural Geology* 14, 963–972.
- Peacock, D.C.P., Sanderson, D.J., 1991. Displacements and evolution of fault segments: example of an extensional fault system at Kilve, Somerset. *Journal of Structural Geology* 13, 721–733.
- Peacock, D.C.P., Sanderson, D.J., 1994. Geometry and development of relay ramps in normal fault systems. *Bulletin of the American Association of Petroleum Geologists* 78, 147–165.
- Peacock, D.C.P., Fisher, Q.J., Willemsse, E.J.M., Aydin, A., 1998. The relationship between faults and pressure solution seams in carbonate rocks and the implications for fluid flow. In: Jones, G., Fisher, Q.J., Knipe, R.J. (Eds.), *Faulting, fault sealing and fluid flow in hydrocarbon reservoirs*. Geological Society, London, Special Publications, vol. 147, pp. 105–115.
- Pedley, H.M., 1978. A new lithostratigraphical and palaeoenvironmental interpretation for the coralline limestone formations (Miocene) of the Maltese Islands. *Overseas Geology and Mineral Resources, H.M.S.O., London*, 54, 17 pp.
- Pedley, H.M., 1987a. Controls on Cenozoic carbonate deposition in the Maltese Islands: review and interpretation. *Memorie della Società Geologica Italiana* 38, 81–94.
- Pedley, H.M., 1987b. The Ghar Lapsi limestones: sedimentology of a Miocene intra-shelf graben. *Centro* 1, 1–14.
- Pedley, H.M., 1990. Syndepositional tectonics affecting Cenozoic and Mesozoic deposition in the Malta and SE Sicily areas (Central Mediterranean)

- and their bearing on Mesozoic reservoir development in N Malta offshore region. *Marine and Petroleum Geology* 7, 171–180.
- Pedley, H.M., 1993. Geological Map of the Islands of Malta, 1:25,000 scale. British Geological Survey, Keyworth, Nottinghamshire, UK.
- Pedley, H.M., 1996. Miocene reef facies of the Pelagian region (central Mediterranean). Models for Carbonate Stratigraphy from Miocene Reef Complexes of the Mediterranean Regions. *SEPM Concepts in Sedimentology and Palaeontology* 5, 247–259.
- Pedley, H.M., 1998. A review of sediment distributions and processes in Oligo-Miocene ramps of S. Italy and Malta (Mediterranean divide). In: Wright, V.P., Burchette, T.P. (Eds.), *Carbonate Ramps*. Geological Society, London, Special Publications, vol. 149, pp. 163–179.
- Pedley, H.M., Bennett, S.M., 1985. Phosphorites, hardgrounds and syndepositional solution subsidence: a paleoenvironmental model from the Miocene of the Maltese Islands. *Sedimentary Geology* 45, 1–34.
- Pedley, H.M., House, M.R., Waugh, B., 1976. The geology of Malta and Gozo. *Proceedings of the Geological Association* 87, 325–341.
- Petit, J.P., Mattauer, M., 1995. Palaeostress superimposition deduced from mesoscale structures in limestone; the Matelles exposure, Languedoc, France. *Journal of Structural Geology* 17, 245–256.
- Reuther, C.-D., Eisbacher, G.H., 1985. Pantelleria Rift: crustal extension in a convergent intraplate setting. *Geologische Rundschau* 74, 585–597.
- Sibson, R.H., 1977. Fault rocks and fault mechanisms. *Journal of the Geological Society*, London 133, 191–213.
- Walsh, J.J., Watterson, J., Bailey, W.R., Childs, C., 1999. Fault relays, bends and branchlines. *Journal of Structural Geology* 20, 1019–1026.
- Walsh, J.J., Bailey, W.R., Childs, C., Nicol, A., Bonson, C.G., 2003. Formation of segmented normal faults: a 3-D perspective. *Journal of Structural Geology* 25, 1251–1262.
- Willemsse, E.J.M., Peacock, D.C.P., Aydin, A., 1997. Nucleation and growth of strike-slip faults in limestone. *Journal of Structural Geology* 19, 1461–1477.
- Yielding, G., Hunsdale, R., 2002. Shale gouge ratio—calibration by geohistory. In: Koestler, A.G. (Ed.), *Hydrocarbon Seal Quantification*. Norwegian Petroleum Society (NPF), Special Publication 11, 1–15.